



Memorandum

Date: April 21, 1999

From: Thomas Prokscha
 Phone: 4275
 Loc.: WLGA/B15
 E-Mail: thomas.prokscha@psi.ch

To: LEM collaboration

cc:

GEANT simulation for e^+ detection in the LE- μ^+ setup at PSI

A simulation of the positrons originating from the LE- μ^+ beam decaying in flight or stopped in the sample (or MCP2 - detector) was performed in order to study

- the asymmetry for the LE- μ^+ setup for a μ^+ polarization of 100%. Using this asymmetry the absolute LE- μ^+ polarization can be determined by comparing with the maximum experimental asymmetry.
- the acceptance of the detectors for decay- e^+ with MCP2 or sample mounted. The simulation will show that there is a decrease of e^+ acceptance of about 35% for the sample mounted on the cryostat compared to the MCP2 detector. This is due to the material (Cu) of the sample holder. Positrons emitted into the downstream direction have to pass several cm of Cu and they are therefore most probably absorbed in the Cu.
- the “phase problem” in the parallel B-field experiment (YBCO). The expected phase difference of 180° between Left and Right detectors was reduced to about 137° (for $T > T_c$ measurements) in the experiment. This is well reproduced by the simulation and is also due to the material of the cryostat.
- the broad “peak” in the decay spectra at times before the muons are implanted into the sample. This peak is more pronounced for the sample cryostat. Again, this is caused by the larger amount of material in the cryostat.
- the change of the α parameter when the beam spot is off centered ($\alpha = N_L(0)/N_R(0)$, where $N_{L,R}(0)$ is the number of events in the L,R spectrum at time zero).

I used the CERN GEANT 3.21 release for the simulation of the interaction of the decay positrons with the material of the LE- μ^+ setup. The advantage of GEANT is the almost “realistic” treatment of particle interactions with matter, including particle decay and generation of secondary particles. Regarding the decay e^+ it is important to account for the energy loss and angular scattering of the e^+ when traversing the material of the apparatus before reaching the detectors. The smearing of the angular distribution of the e^+ yields a decrease of the observable decay asymmetry. Also, a non-zero energy deposition in the detectors has to be required in order to “see” the e^+ in the detectors. GEANT treats each particle passing a detector as a hit but it is necessary to check, that the particle deposits energy in the detector.

The generation of secondary particles due to decay- e^+ is caused by the γ -production by Bremsstrahlung or annihilation in flight. These γ ’s may generate $e^+ e^-$ pairs which also may hit the

detectors. So, one can play with the start parameters of the simulation (generation of secondary particles or not, lower cut energies E_{low} for the particles: if $E < E_{low}$ particle stops) and look for the effects on the total number of detected e^+ and the decay asymmetry. I will show the results for

- only e^+ generation with $E_{low} = 100$ keV.
- generation of γ , $e^- e^+$ pairs allowed with $E_{low} = 100$ keV for all kinds of particles. For $E_{low} > 100$ keV the acceptances for e^+ are between the options ‘secondary particles with $E_{low} = 100$ keV’ and ‘only e^+ with $E_{low} = 100$ keV’.

Later, we will see that the detection efficiency for γ ’s is negligible since the energy deposited in the scintillators is lower than 100 keV.

The Monte-Carlo simulation program GEANT.LEMSR.FOR is located on the PSI OpenVMS cluster in the directory DISK_142_SRC0:[PROKSCHA.MC.SRC]. Compile and link the program with the DCL procedure GEANT.LEMSR.BLD.COM in the same directory. The steering of the program can be done interactively after starting the program or by using an input file (GEANT.LEMSR.INPUT in [PROKSCHA.MC.INP]) which can be read by the program. When using the graphical output option the detector with particle tracks is shown as well as the GEANT HITS data bank for each detector. For large numbers of particles to be thrown a DCL routine for running in batch mode is available (GEANT.LEMSR.BATCH.COM in [PROKSCHA.MC.COM]). The maximum CPU time for 500 k events is about 20 min on the cluster (PSICL0 or PSICL1). The output data are written to Ntuples which have a minimum size of 37 Mb for 500 k events. The number of Ntuple variables is selectable in the input file or interactively. The single decay spectra are obtained by applying several cuts to the Ntuple data using the PAW analysis program. A PAW macro doing the job is available (in directory [PROKSCHA.PAW] the .KUMAC’s GEANT.DOHIST, GEANT.DOHIST2 and .GEANT_ELOSS; the first two macros are for filling of decay spectra and getting the total acceptance of the detectors, the last one plots the energy losses of the particles in the detectors). To compile, link and run the program the logicals mc\$src, mc\$out, mc\$exe, and mc\$inp must be defined: mc\$src is the source directory for the program code, mc\$out is the output directory, mc\$exe contains the EXE file, and the input file is located in mc\$inp.

A drawing of the LE- μ^+ setup used in the program is shown in Fig. 1a) and 1b). The cryostat without coldfinger and sample is simplified by a $\phi_a = 3\text{-cm}$ -Cu tube with a $\phi_i = 1\text{-cm}$ -vacuum cylinder inside for the He. However, the correct dimension of the inner parts are unknown. Also, the guard rings of the acceleration stage are not implemented. Figure 2a) and 2b) shows the setup with the cryostat substituted by the MCP2 detector. The reference system is indicated with z-axis parallel to the beam axis. The origin of the reference system is in the center of the “MCP2-vacuum tube”, the DN160 tube at the end of the beam line. The surface of the sample or the MCP2 is at $z = 1.4$ cm, a bit downstream with respect to the center of the tube. There is the possibility to generate particles at

- “ $z = 0$ ”, which means in the sample at $z = 1.40002$ cm, 200 nm deep. This option is used to determine e^+ acceptances, decay asymmetries and to study the “phase problem” in B-parallel measurements.
- negative z , this is upstream of the target. This option is used to look for the peak in the decay spectra just before the μ^+ are implanted. Muons are started at $z = -74$ cm with momenta of 1.62 MeV/c and 1.95 MeV/c, corresponding to μ^+ energies of 12.4 keV and 18 keV, respectively. Each value of momentum and z can be chosen; however, the lowest possible energy for particles in GEANT is 10 keV, corresponding to a μ^+ momentum of 1.45 MeV/c. Additionally, a divergence of the beam can be entered in this case. If a B-field is applied it is handled for the μ^+ spin precession as a homogenous field during the total path of the μ^+ , but has no influence on the μ^+ trajectory.

The generated beam spot is isotropic with an diameter of 2 cm. At the moment, a B-field parallel

to y or parallel to z can be applied, but not B_y and B_z components simultaneously.

GEANT data for e^+ acceptances, decay asymmetries and comparison with experimental data

As it was pointed out above the energy deposited in the detectors by γ 's is mainly lower than 100 keV, see Fig. 3. The e^+ energy loss peaks at about 1 MeV. This is expected for minimum ionizing particles which have for low Z materials a stopping power of $dE/dx \sim 2\text{MeV}/(\text{g/cm}^2)$. This gives $dE = 1\text{ MeV}$ for each scintillator with $l = 0.5\text{ cm}$ and $\rho = 1\text{ g/cm}^3$, in agreement with the simulation.

Now, we will look for acceptances and decay asymmetries for sample and MCP2 mounted, respectively. The results are summarized in Tab. 1.

Oooh, what are all these numbers ?

1. The first column should be clear, it's the setup used in the simulation. The simulation is for 500 k e^+ started at the sample or MCP2.
2. The second column gives the secondary particles used in the simulation and the lower cut energy. If the energy of the particle is lower than the cut energy the particle stops.
3. Hits > 0: this is the fraction (compared to the 500 k started e^+) of particles traversing the detectors. Remember, GEANT counts a Hit although there might be no energy deposited in the detectors. For the first four rows this fraction is close to 90% due to the large number of γ 's created in the sample.
4. Hits > 0 and $dE > 0$: now, an energy loss > 0 is required, but γ 's are included. The A's are fitted asymmetries for a 50 G transversal field. The subscript o(=only) means that there was only one hit in one single pair of detectors. The subscript a(=all) means that there could be also another hit in another detector.
5. Hits > 0, $dE > 0$, e^+ or e^- : the same as 4. But now, require that a hit contains at least a e^+ or e^- . **These are the right numbers assuming that the γ 's are not detected.** Here, the meaning of the subscript o(=only) is different to that in 4.: there was only one hit in a detector with energy deposition in this detector, and there may be other hits in other detectors but with no energy deposited (so, we didn't detect this hit).
6. Some experimental data. Asymmetries are from Run 1892-1896 (400 nm Au), fitted with exponential damping ($\lambda = 0.02(4)\mu\text{s}^{-1}$) and cut on the slow μ^+ peak in the M3S1 multi - hit - TOF spectra. The 'only' data are obtained by cutting on the IO506 spectrum.
The ϵ_{e^+} are the measured positron detection efficiencies with MCP2 mounted.

The fractions N_o/N_a are the ratios of entries in the decay spectra for the 'only' and 'all' cuts.

Table 1: Simulated and experimental e^+ efficiencies and decay asymmetries. See text for details.

Setup	particles	Hits > 0	Hits > 0 dE > 0	Hits > 0 dE > 0 e^+ or e^-	Experiment
Run XI cryo	e^+, e^-, γ $E_{low} = 100$ keV	93.66% $\frac{N_o}{N_a} = 76.4\%$ $\frac{N1_o}{N1_a} = 98.5\%$	41.38% $A_o = 29.35(35)\%$ $A_a = 28.14(31)\%$	38.73% $A1_o = 29.00(32)\%$ $A1_a = 28.90(31)\%$	$A_o^{exp} = 26.37(31)$ $A_a^{exp} = 26.26(29)$ $\frac{N_o^{exp}}{N_a^{exp}} = 97.1\%$
Run XI MCP2	e^+, e^-, γ $E_{low} = 100$ keV	89.88% $\frac{N_o}{N_a} = 81.9\%$ $\frac{N1_o}{N1_a} = 98.9\%$	60.55% $A_o = 29.77(28)\%$ $A_a = 29.09(25)\%$	59.00% $A1_o = 29.42(25)\%$ $A1_a = 29.33(25)\%$	$\epsilon_{e^+} = 58.1(1.3)$ $\frac{N_o^{exp}}{N_a^{exp}} = 97.5\%$
Run X MCP2 WSZ anode	e^+, e^-, γ $E_{low} = 100$ keV	88.24% $\frac{N_o}{N_a} = 83.41\%$	65.32% $A_o = 29.76(26)\%$ $A_a = 29.13(24)\%$	64.21% $A1_a = 29.33(24)\%$	$\epsilon_{e^+} = 61.7(1.1)$
Run XI cryo Al, 1mm He-shield	e^+, e^-, γ $E_{low} = 100$ keV	93.96% $\frac{N_o}{N_a} = 79.3\%$ $\frac{N1_o}{N1_a} = 98.5\%$	51.89% $A_o = 31.29(36)\%$ $A_a = 30.70(27)\%$	49.81% $A1_o = 31.17(28)\%$ $A1_a = 31.11(27)\%$	Possible Improvement
Run XI cryo	e^+ $E_{low} = 100$ keV	37.08% $\frac{N_o}{N_a} = 98.1\%$ $\frac{N1_o}{N1_a} = 99.9\%$	35.30% $A_o = 29.42(33)\%$ $A_a = 29.18(32)\%$	35.30% $A1_o = 29.17(33)\%$ $A1_a = 29.18(32)\%$	$A_o^{exp} = 26.37(31)$ $A_a^{exp} = 26.26(29)$ $\frac{N_o^{exp}}{N_a^{exp}} = 97.1\%$
Run XI MCP2	e^+ $E_{low} = 100$ keV	59.32% $\frac{N_o}{N_a} = 98.35\%$ $\frac{N1_o}{N1_a} = 99.93\%$	56.47% $A_o = 29.61(26)\%$ $A_a = 29.42(26)\%$	56.47% $A1_o = 29.43(26)\%$ $A1_a = 29.42(26)\%$	$\epsilon_{e^+} = 58.1(1.3)$ $\frac{N_o^{exp}}{N_a^{exp}} = 97.5\%$
Run X MCP2 WSZ anode	e^+ $E_{low} = 100$ keV	65.55% $\frac{N_o}{N_a} = 98.32\%$	62.39% $A_o = 29.52(25)\%$ $A_a = 29.36(25)\%$	62.39% $A1_o = 29.37(25)\%$ $A1_a = 29.36(25)\%$	$\epsilon_{e^+} = 61.7(1.1)$
Run XI cryo Al, 1mm He-shield	e^+ $E_{low} = 100$ keV	49.45% $\frac{N_o}{N_a} = 98.1\%$ $\frac{N1_o}{N1_a} = 99.9\%$	47.17% $A_o = 31.53(28)\%$ $A_a = 31.23(28)\%$	47.17% $A1_o = 31.26(28)\%$ $A1_a = 31.23(28)\%$	Possible Improvement
no material only 100k e^+	e^+ $E_{low} = 100$ keV	82.16% == solid angle	80.05% $A_o = 26.3(5)\%$ $A_a = 26.3(5)\%$	80.05%	

Now, for simplicity, I will focus only on the 5. column, thus assuming that γ 's are not detected. Then, I skip the data where 'only e^+ ' are handled in the simulation, since the measured $\epsilon_{e^+} = 58.1(1.3)\%$ is in some contradiction to the GEANT $\epsilon_{e^+} = 56.47\%$. So, I use only the **bold** numbers. However, all conclusion will hold within a relative error of a few percent, if one would use also the 4.column and the 'only e^+ ' data.

- **Absolute μ^+ polarization.** This is obtained by dividing the experimental by the simulated asymmetries:

$$P_\mu = 26.37(31)/29.00(32) = 90.9(1.5)\%,$$

$$P_\mu = 26.26(29)/28.90(31) = 90.9(1.5)\%.$$

However, there might be a depolarization due to Mu formation at the trigger foil. Assuming 5% Mu formation for 20 keV μ^+ , the fraction of Mu reaching the sample plane should be about 3% (this is for RunX geometry by program MUTRACK). The μ^+ from these Mu atoms are out of phase with the dominant μ^+ fraction and therefore, they can not contribute to the wiggles. Assuming an equal detection probability for the Mu atom reaching the sample plane, the μ^+ polarization at the trigger foil is then $90.9/0.97\% = 93.7\%$.

- **Positron detection efficiency for sample compared to MCP2 in RunXI:**

$$\epsilon_{e^+}^{sample}/\epsilon_{e^+}^{MCP2} = 38.73/59.00 = 65.6\%.$$

So, if we use the experimental $\epsilon_{e^+}^{MCP2} = 58.1(1.3)\%$, then the **absolute positron detection efficiency with sample** is only

$$\epsilon_{e^+}^{sample} = 38.1(9)\% !$$

The maximum detected μ^+ rate in Run XI was about 80/s (including a fraction of about 10% of "fast" μ^+). The total LE- μ^+ rate N_μ^{sample} at the sample is then

$$N_\mu^{sample} = 0.9 \cdot 80/s \cdot 1/(\epsilon_{e^+}^{sample} \cdot \epsilon_{TD}) = 72/s/(0.381 \cdot 0.8) = 236/s,$$

where $\epsilon_{TD} \sim 80\%$ is the trigger detection efficiency. With a simulated transport efficiency of 42% we obtain the LE- μ^+ rate $N_\mu^{mod} = 560/s$ at the moderator (with an incoming muon beam rate of $\sim 1.7 \cdot 10^7/s$).

The $\epsilon_{e^+}^{MCP2} = 61.7\%$ for the WSZ anode was higher than for the new Delay-Line anode due to additional e^+ absorption in the thick stainless steel anode of the Delay-Line detector.

- **But we can improve it !**

By substituting the Cu sample holder ring and the two Cu plates (4 mm and 5 mm thick) at the sapphire plate by Al, and by reducing the thickness of the He-shield from 2 mm to 1 mm, the absorption of e^+ can be reduced and the simulation predicts also an increase of asymmetry:

$$\text{Gain in } e^+ \text{ detection efficiency} = 49.81/38.73 = 1.28.$$

$$\epsilon_{e^+}^{sample}(\text{Al plates}) = 49.0(1.1)\%.$$

$$\text{Gain in asymmetry} = 31.1/29.0 = 1.07.$$

The detected μ^+ rate should increase from 80/s to about 100/s.

Some final remarks to the strong e^+ absorption in Cu: can it be ? Oh yes, indeed: let's have a look on the radiation length of e^+ in Cu, it is 1.4 cm. What does the radiation length mean ? It is the length where a e^+ losses $(1-1/e) = 63\%$ of its energy by radiation processes. These processes compete with energy loss by ionization and become dominant in Cu for e^+ -energies larger than 20 MeV ($= 590/Z$ MeV, with Z the nuclear charge). The main fraction of the Michel spectrum has higher energies. The e^+ emitted in the half-space downstream of the sample have to cross several radiation lengths before they leave the Cu; so, they are most probably absorbed. Al is better, because its radiation length is 8.9 cm and also the energy of 45 MeV, where radiation processes

become dominant, is higher.

The Left-Right phase difference in the B-parallel measurement

In the B-field parallel experiment the observed phase difference between L and R spectra was only 137 degree ($T > T_c$ runs) instead of 180 degree. This is also due to the Cu in the sample holder. I made a simulation without any material which gives an asymmetry of about 27%, wiggles in L and R and no wiggles in T and B, as expected, see Fig. 4a). The phase difference is 180 degree. With the Run XI cryo setup the phase difference becomes 134 degree and the asymmetry should be about 31%, a bit higher than 29% for the measurements with B perpendicular to the sample, see Fig. 4b). The surprising feature is the occurrence of wiggles in the T and B spectra (which we didn't have in our experiment). The phases of T and B are the same and the asymmetry is about 15%, and the phases are shifted by 90 degree with respect to the initial phase of L, which is 0 degree without material in the simulation. This is explained by the fact, that, if the spin directs towards the cryostat the decay e^+ have more material to cross in order to reach T or B than for the case of opposite spin direction. This causes a modulation in the detection efficiency for the T and B detectors.

The shape of the decay spectra before time zero

There is a broad peak observable in the decay spectra just before time zero t_0 , the average time of implantation. Data are shown for Runs 1892 - 1896 (400 nm gold, 20 kV at moderator, sample was always set to 0 kV) in Fig. 5a) (online cut on slow muon peak in M3S1 multi-hit TOF spectra) and in Fig. 5b) without cuts. The peak is well reproduced by the GEANT simulation, Fig. 5c), where the μ^+ started 74 cm upstream of the sample with an energy of 18 keV. At the moment, no energy spread is included in the simulation. Similar data are shown for the Runs 1898 - 1902 (15 kV at the moderator) in Fig. 6a)-c). The data with MCP2 instead of sample are shown in Fig. 7a)-c).

Qualitatively, the peak is well reproduced by the simulation for the sample and MCP2 data. For the MCP2 data there is nearly no peak observable, both in data and simulation. The peak is most pronounced for the 20 kV data on sample. And, the peak is located definitely at times before the μ^+ are implanted. This is due to the larger acceptance of the downstream - half of the paddles for decay positrons, if these positrons are emitted just a few cm before the μ^+ hits the sample. For example, at $t = t_0 - 10$ ns the distance of the μ^+ is about 5 cm. They have at this distance a 'good view' onto the whole spectrometer and therefore, the detection probability is high. Once they are implanted, about half of the spectrometer is invisible for the e^+ , causing the decrease of event rate at $t \geq t_0$. The rise, starting at channel 950, is due to the increasing solid angle of the spectrometer when the μ^+ are approaching the sample.

The shape of the increasing part of the spectrum is gaussian to good approximation, which can be seen when fitting a gaussian to the broad peak, see Figs. 5-7. The experimental data without cut have a larger σ than the ones with TOF cut. For example, $\sigma = 26.2$ ns for 20 kV data with cut [see Fig. 5a)] and $\sigma = 29.5$ ns for data without cut [see Fig. 5b)]. Without cut there are always fast μ^+ contributing to the decay spectra with a different TOF distribution, thus giving a broader TOF distribution. This can be also seen when comparing the 15 kV data (Fig. 6) with the 20 kV data: the 15 kV data have larger σ 's due to the broader TOF distribution compared to the 20 kV data, see the M3M2 TOF-spectra shown in Figs. 8c)-8d). The energy bite for the LE- μ^+ after the trigger detector is for both cases nearly the same (~ 500 eV); since the 15 keV μ^+ are slower the TOF-distribution for a fixed length becomes broader compared to 20 keV μ^+ (you can check this by writing the energy-time relation, you will find $\Delta t \propto \Delta E \cdot t^3$: the longer the TOF t the larger the width Δt of the TOF distribution for a given energy width ΔE). The simulated data (mono-energetic !), for 20 kV give a $\sigma = 15.3$ ns [see Fig. 5c)] and $\sigma = 20.1$ ns for the 15 kV settings [see Fig. 6c)]. The μ^+ for the 15 kV setting are slower and therefore, the solid angle increases slower when approaching the sample yielding a smearing out of the time dependent detector acceptance

for the μ^+ decaying in flight.

The experimental σ 's are much larger than the simulated. One explanation is the use of a mono-energetic beam in the simulation. However, I would expect naively, that the experimental σ can be calculated by adding quadratically the simulated σ and the width of the experimental M3M2-TOF distribution (this results when folding the simulated data with a gaussian TOF-distribution). But this does not work: for the 20(15) kV, in order to obtain the experimental $\sigma = 26.2(33.5)$ ns from the simulated $\sigma = 15.3(20.1)$ ns, one needs a TOF- $\sigma = \sqrt{26.2^2 - 15.3^2} = 21$ ns, and 26.8 ns for the 15 kV data ! If I fit a gaussian to the total M3M2-TOF spectra including the fast μ^+ I get TOF- $\sigma = 9.6(12.5)$ ns for 20(15) kV, too low...

The simple formula above seems to work not properly: I folded the simulated decay spectra with different gaussians and fitted the folded spectra; to obtain the experimental σ 's I have to use a gaussian with $\sigma_{fold} = 16(22)$ ns for the 20(15) kV data, see Fig. 9. Still too broad... The best thing to do would be a simulation with the real energy distribution in the LE- μ^+ beam, but this will take some time to implement the changes in the program.

In Fig. 8a) and b) decay spectra with TOF cuts in M3S1 and M3M2 are shown. The cut intervals are shown in Fig. 8c) and d). When cutting on the μ^+ in M3M2 the decay spectrum begins later (hatched areas) ! This is well reproduced by the simulated spectrum in Fig. 8e). The reason is, that we now require a hit on the MCP2: a μ^+ decaying in flight upstream of the MCP2 cannot produce a hit in both MCP2 and scintillators (more precisely: only with a small probability a hit is possible, if the decay e^+ hits MCP2, deposits energy and is scattered towards the scintillators); if a hit in MCP2 is required nearly all μ^+ decaying in flight are rejected which leads to the start of the decay spectra at implantation time.

The α parameter when shifting the beam spot off center

For this study I used a smaller beam spot with a diameter of 1 cm, but again homogeneously distributed. A B-field of 50 G was applied parallel to the beam axis and the center of the beam spot was shifted by 0,1,2,3,5 mm towards the L detector (this is in x-direction in the simulation). The simulated spectra were fitted to obtain the number of events at time zero $N_{L,R}(0)$ for the L and R spectrum. The results are shown in Fig. 10, where the ordinate just gives $\alpha = N_L(0)/N_R(0)$. The data points can be fitted by a second order polynom, so some extrapolation to other shifts than those used above is possible.

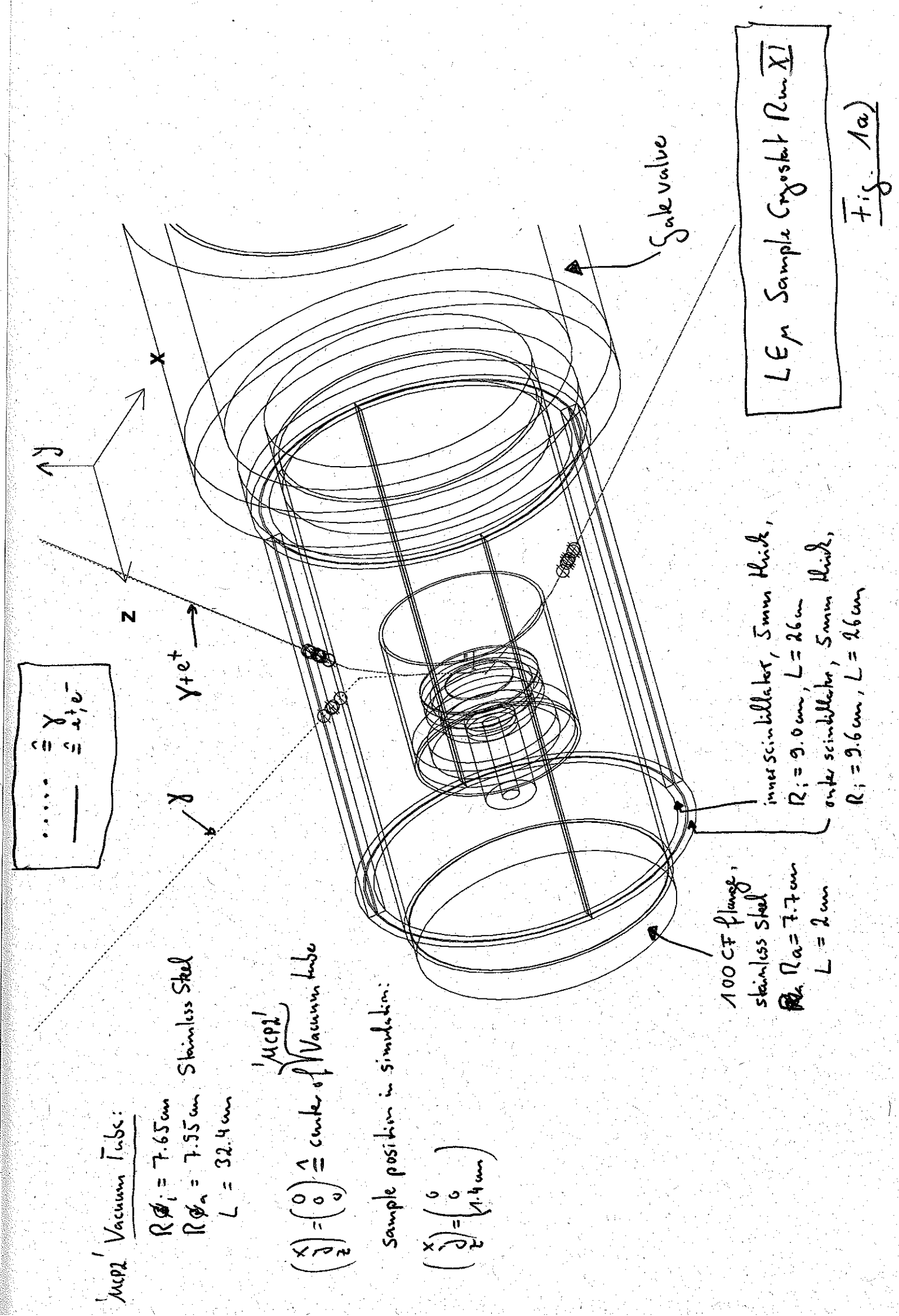
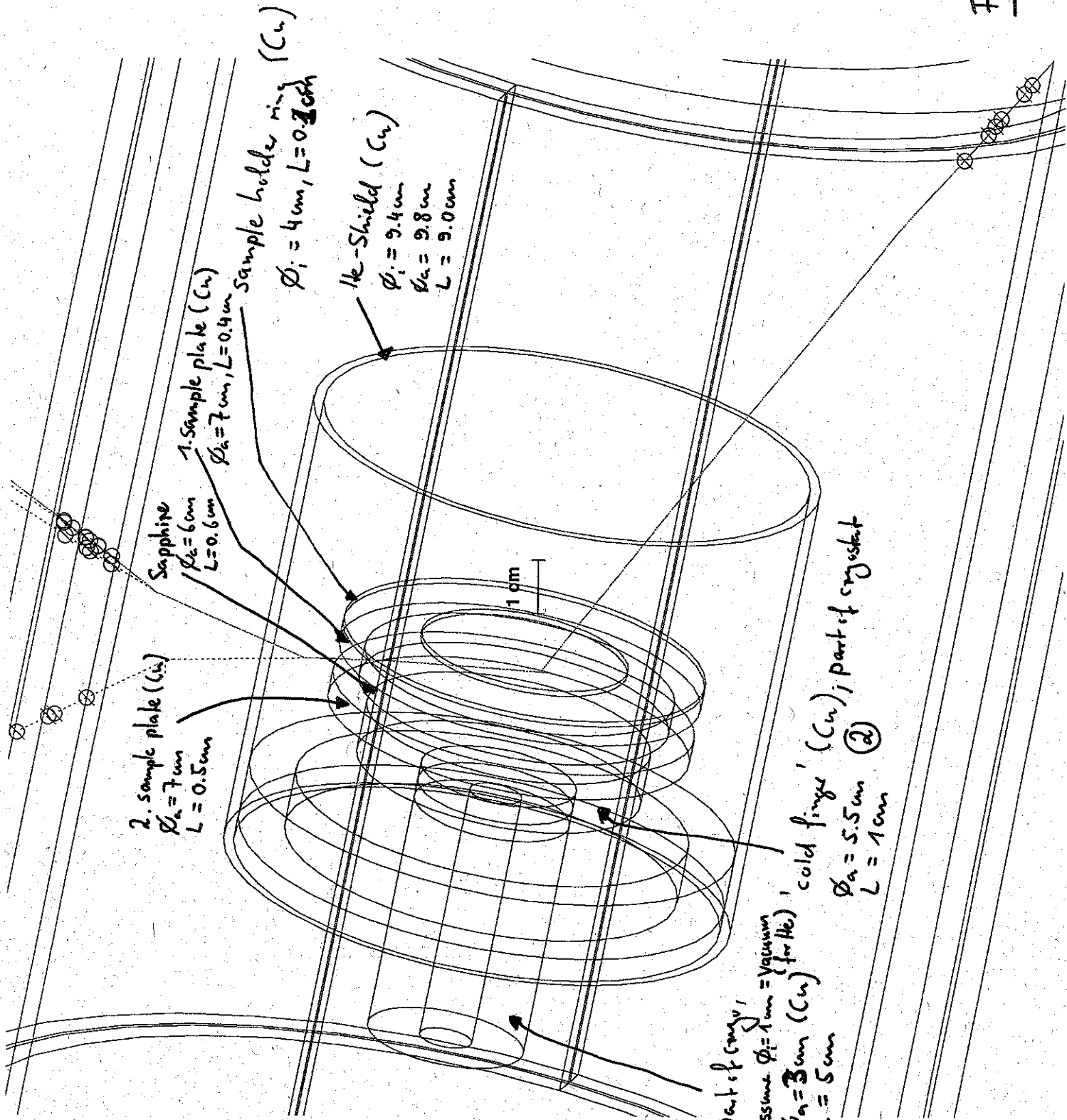
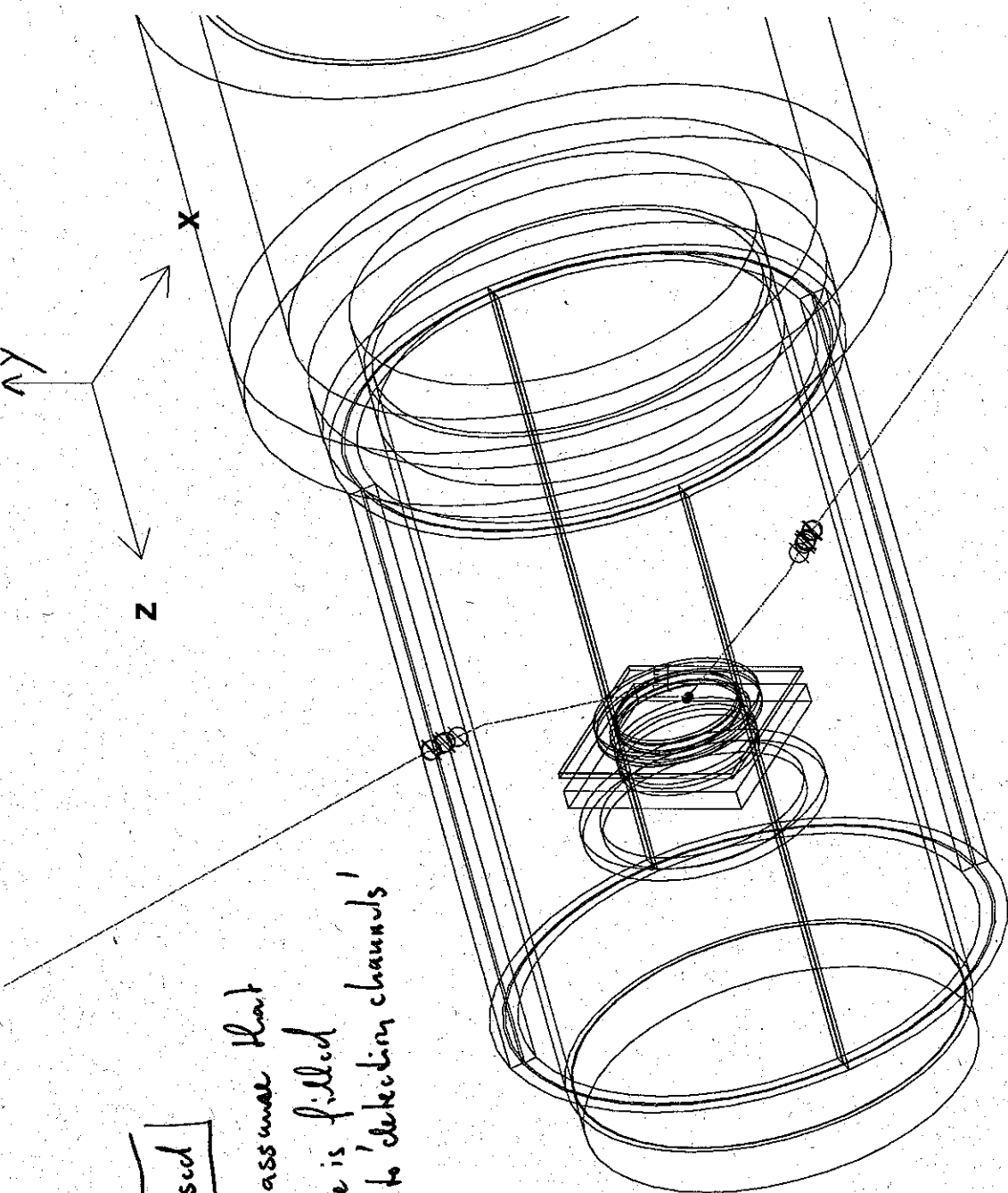


Fig. 1b)



① = part of congi,
assume $D_i = 1 \text{ cm} = \text{vacuum}$,
 $D_o = 3 \text{ cm} (\text{Cu})$, 'cold finger' (Cu), part of congi stat
 $D_o = 5 \text{ cm}$ ②
 $L = 1 \text{ cm}$

Cu plate,
 $D_o = 3 \text{ cm}$
 $L = 0.7 \text{ cm}$



$S_{\text{upr}} = 2 \text{ g/cm}^3$ used

$\rho_{\text{supg}} = 4.5 \text{ g/cm}^3$; assume that
only 50% of volume is filled
with MCP glass due to 'delection channels'

Fig. 2a)

MCP2 detector Run XI,
Delay Line anode

MCPs: $\rho_a = 5\text{ cm}$ $L = 0.3\text{ cm}$ (3 Galileo MCP's)

2 MCP holder rings
(Ceramic, use Alcor)

$$\begin{aligned}\rho_i &= 4.8\text{ cm} \\ \rho_a &= 6.5\text{ cm} \\ L &= 0.15\text{ cm}\end{aligned}$$

Support Rings:
 $\rho_i = 8.0\text{ cm}$
 $\rho_a = 9.6\text{ cm}$
 $L = 0.5\text{ cm}$

Stainless Steel
anode

$$\begin{aligned}L_x &= L_y = 7.3\text{ cm} \\ L_z &= L = 0.8\text{ cm}\end{aligned}$$

$$\begin{aligned}\rho_i &= 5.5\text{ cm} \\ L &= 0.3\text{ cm}\end{aligned}$$

in center: $L_z = 0.2\text{ cm}$
at end: $L_z = 0.2\text{ cm}$

\Rightarrow thickness of anode in center = 0.2 cm!

Stainless Steel mounting plate

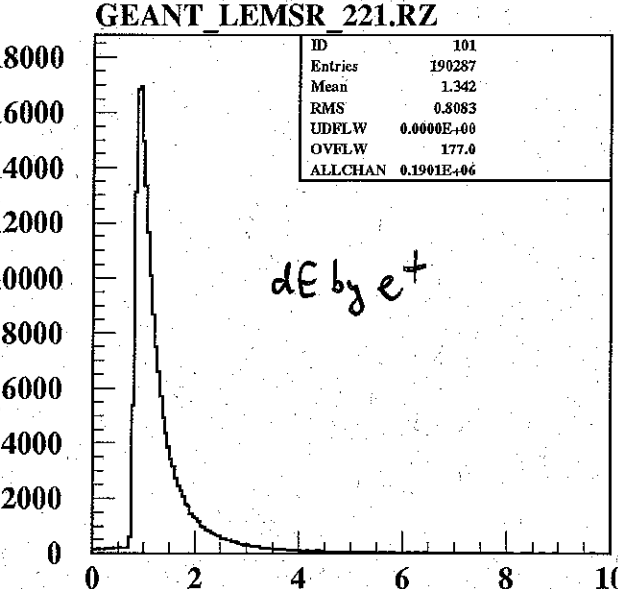
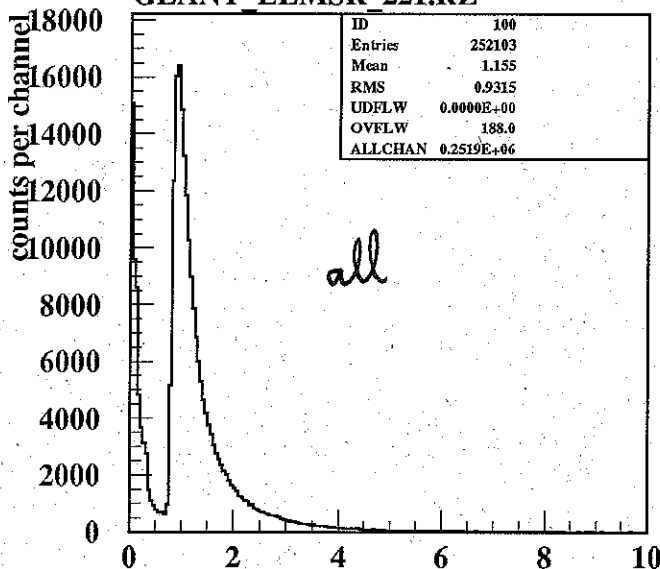
$$\begin{aligned}\rho_i &= 5.5\text{ cm vacuum} \\ L_x &= L_y = 7.3\text{ cm} \\ L &= L_z = 0.2\text{ cm}\end{aligned}$$

Fig 2b:

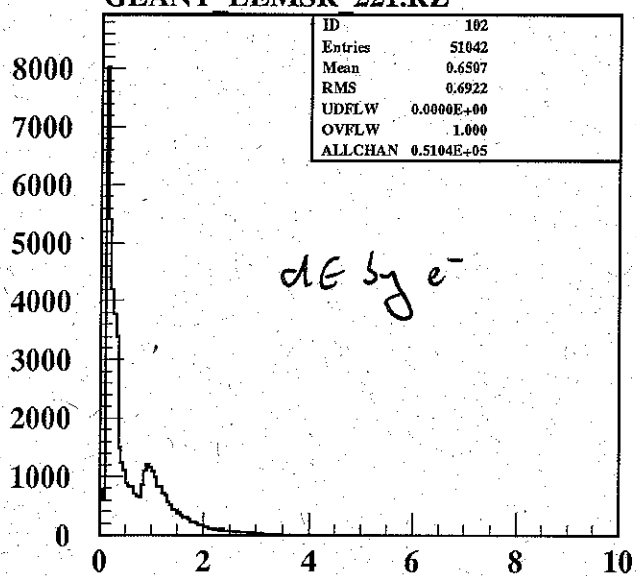
Generation of secondary e^+, e^-, γ 's; $E_{low} = 100\text{keV}$

09/04/99 14.02

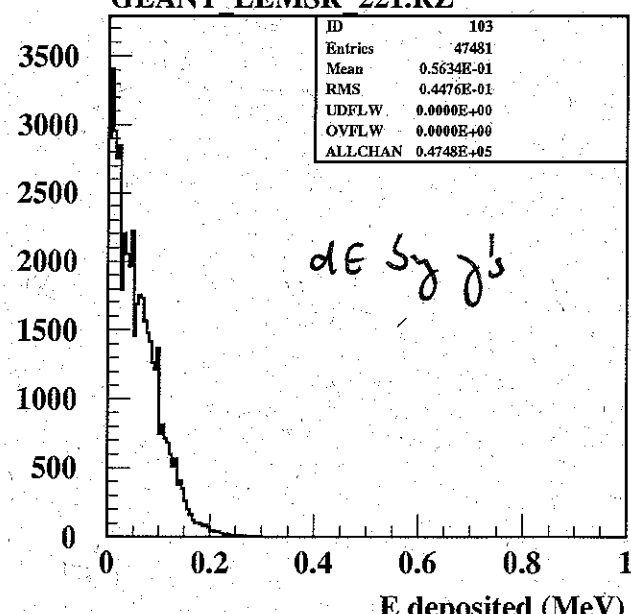
Simulated energy loss in inner scintillators, RunXI cryo setup, 500k e^+
GEANT LEMSR_221.RZ



GEANT LEMSR_221.RZ



GEANT LEMSR_221.RZ



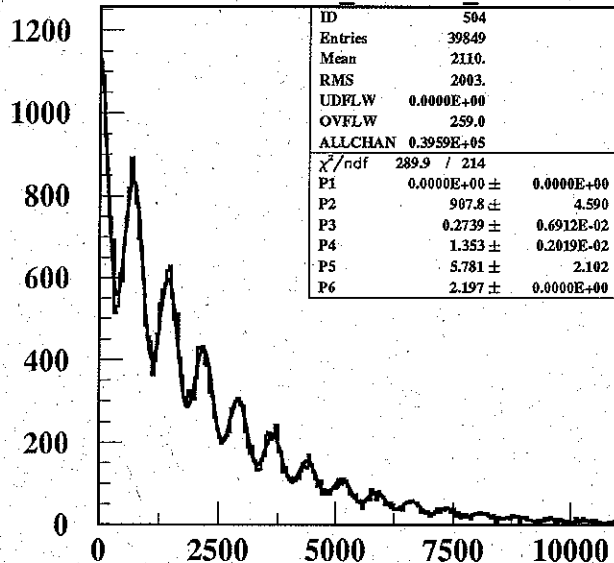
Note, that $\sum_{\text{entries}} 101, 102, 103 > \text{Entries of } 100$; many e^+ and e^- are accompanied by γ 's.

dE changes for γ 's when modifying E_{low} for γ 's; not really understood...

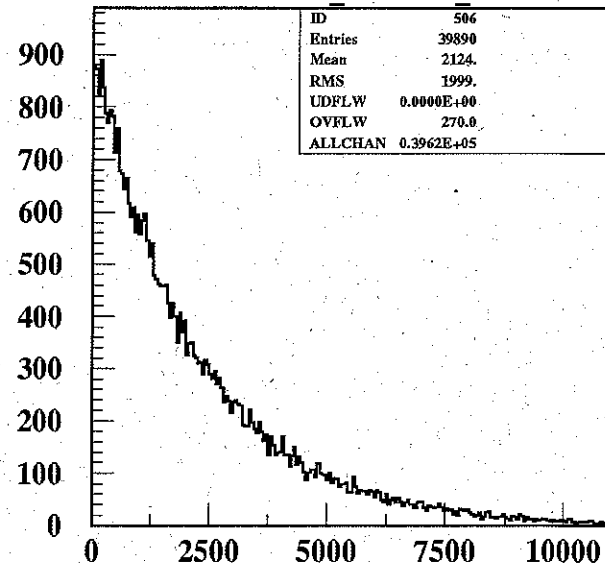
Fig. 3

09/04/99 20.46

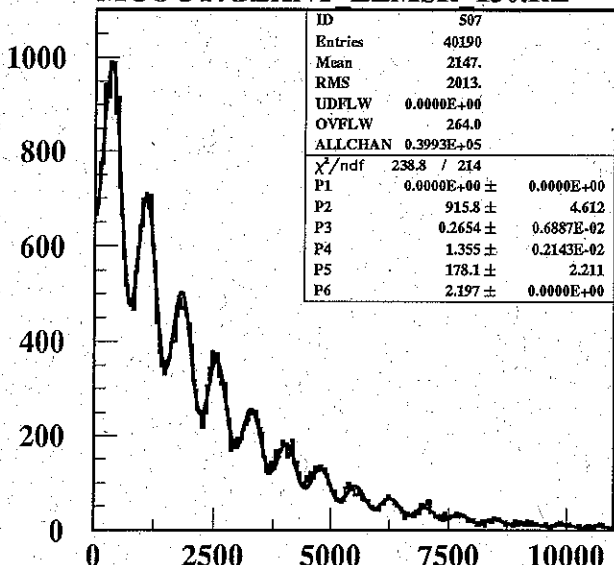
**GEANT, 100 G vertical, e+ at 1.4cm, e+, e-, γ 100 keV, 200 k events
MCOUT:GEANT_LEMSR_150.RZ**



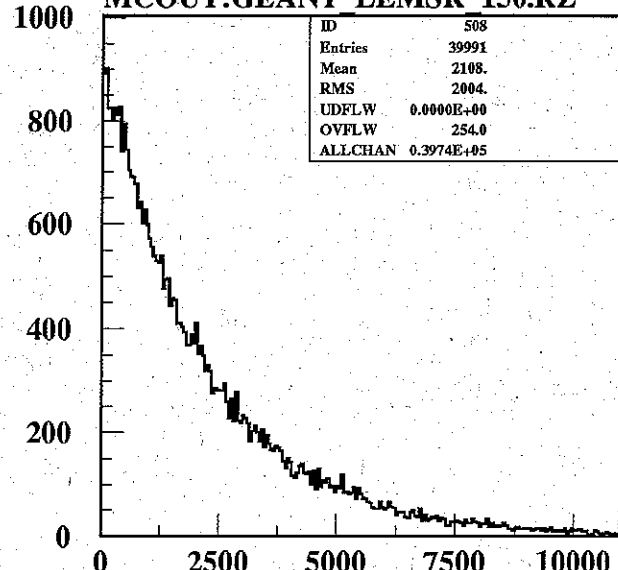
MCOUT:GEANT_LEMSR_150.RZ



**GEANT 150 left , de gt 0, 50ns bins
MCOUT:GEANT LEMSR 150.RZ**



**GEANT 150 top , de gt 0, 50ns bins
MCOUT:GEANT LEMSR 150.RZ**



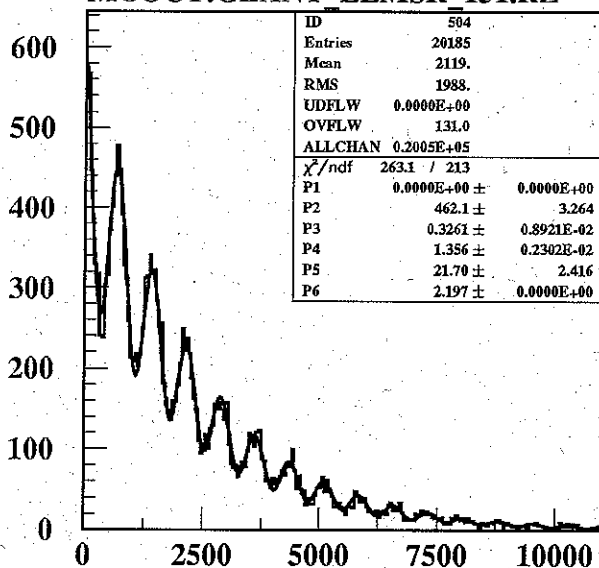
GEANT 150 right, de gt 0, 50ns bins

GEANT 150 bottom, de gt 0, 50ns bins

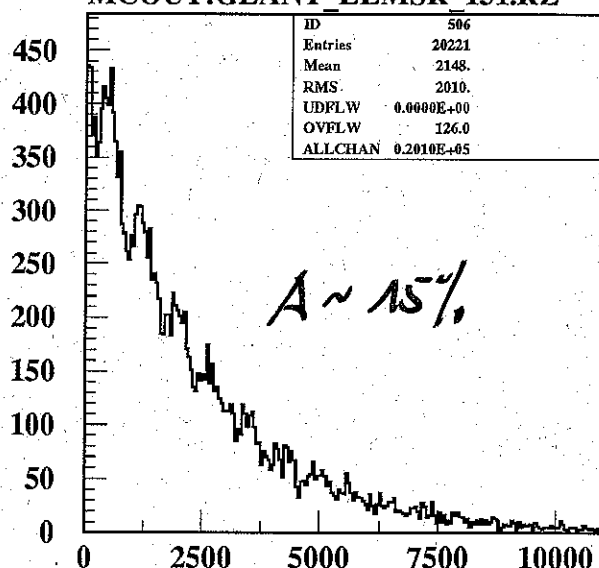
Fig 49)

09/04/99 20.47

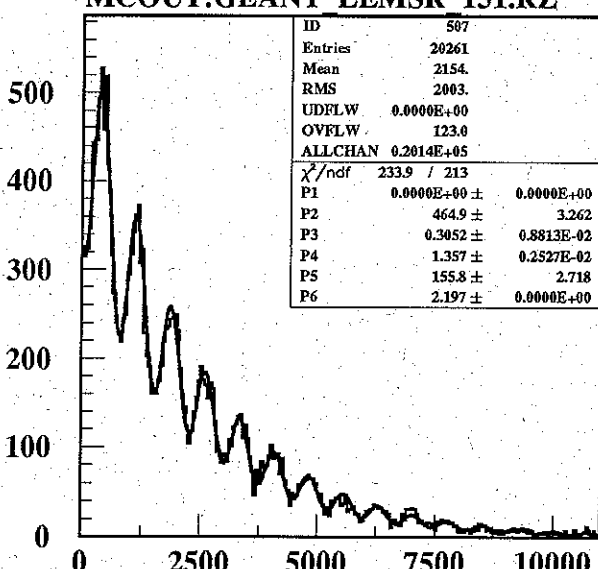
GEANT, 100 G vertical, e+ at 1.4cm, e+, e-, γ 100 keV, 200 k events, RunXI set
MCOUT:GEANT_LEMSR_151.RZ



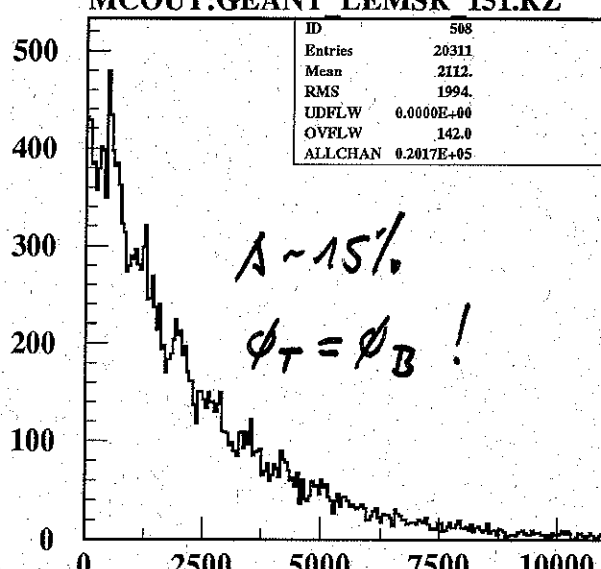
MCOUT:GEANT_LEMSR_151.RZ



GEANT 151 left , de gt 0, 50ns bins
MCOUT:GEANT_LEMSR_151.RZ



GEANT 151 top , de gt 0, 50ns bins
MCOUT:GEANT_LEMSR_151.RZ



GEANT 151 right, de gt 0, 50ns bins

GEANT 151 bottom, de gt 0, 50ns bins

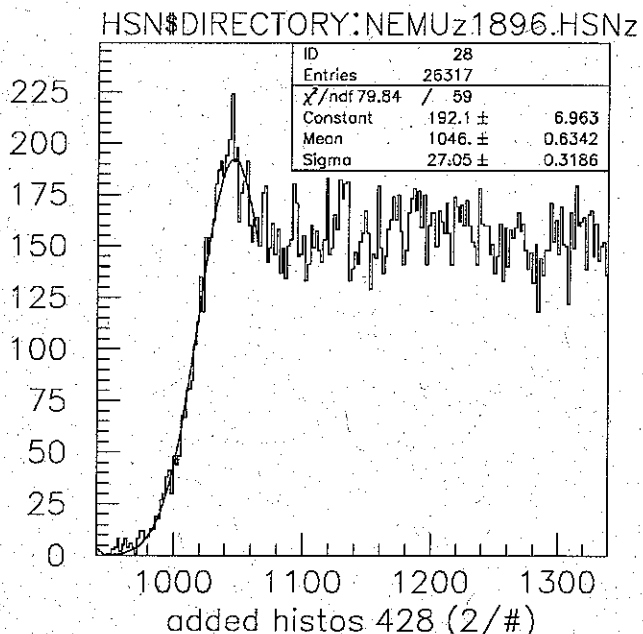
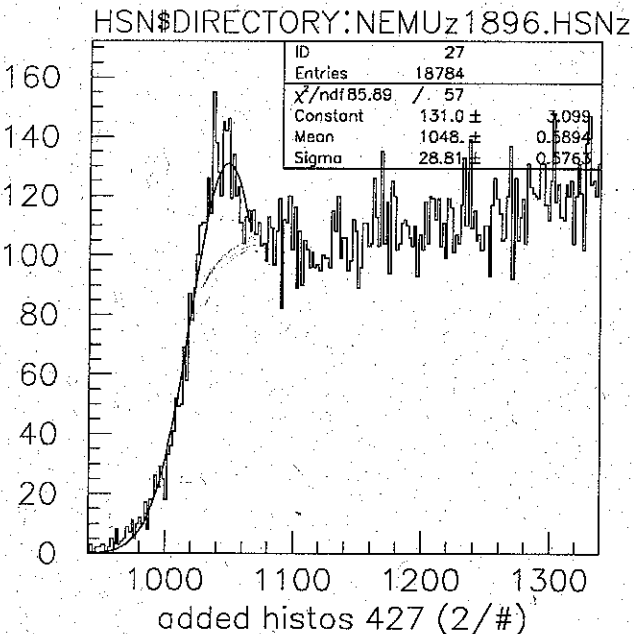
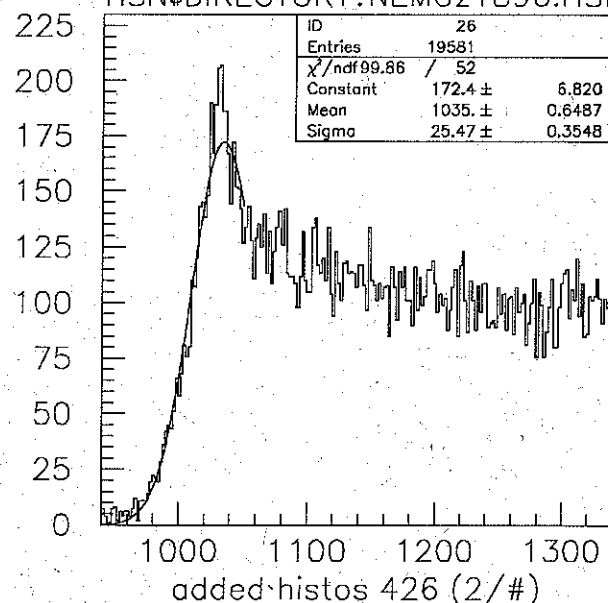
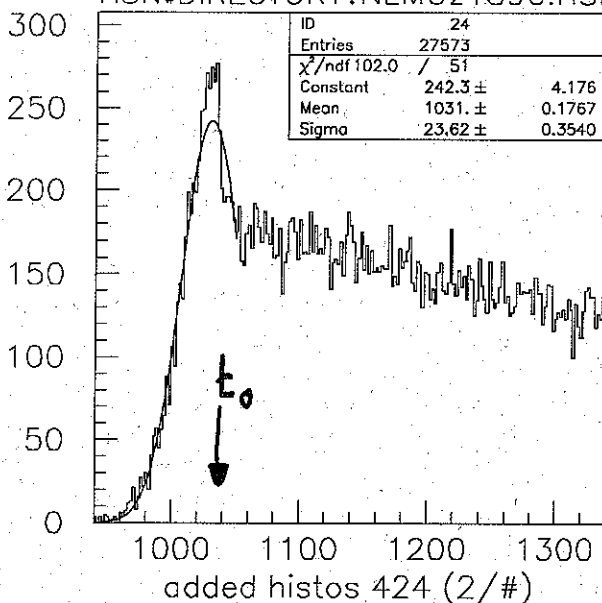
Fig 45

20/04/99 15.26

Run 1892–1896 20kV, 100G, 400nm Au, OnlineM3S1cut(90–108), Sample 0kV

HSN\$DIRECTORY:NEMUz1896.HSNz

HSN\$DIRECTORY:NEMUz1896.HSNz



$$\bar{\sigma} = 26.2 (1.1) \text{ ns}$$

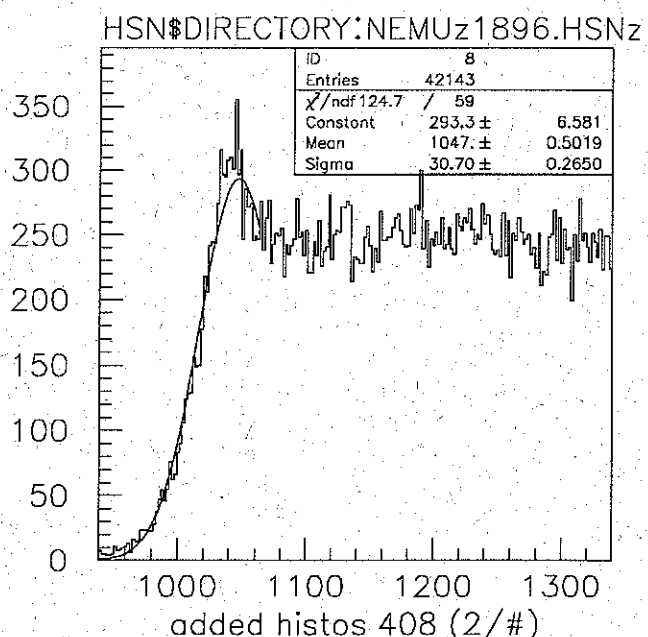
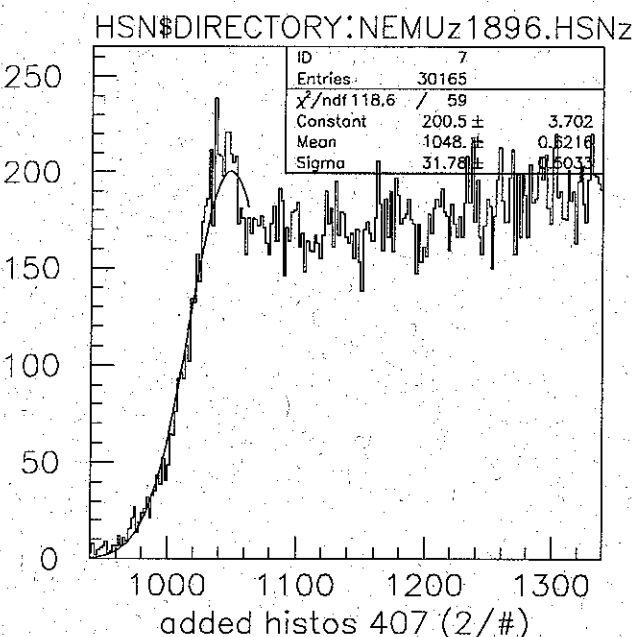
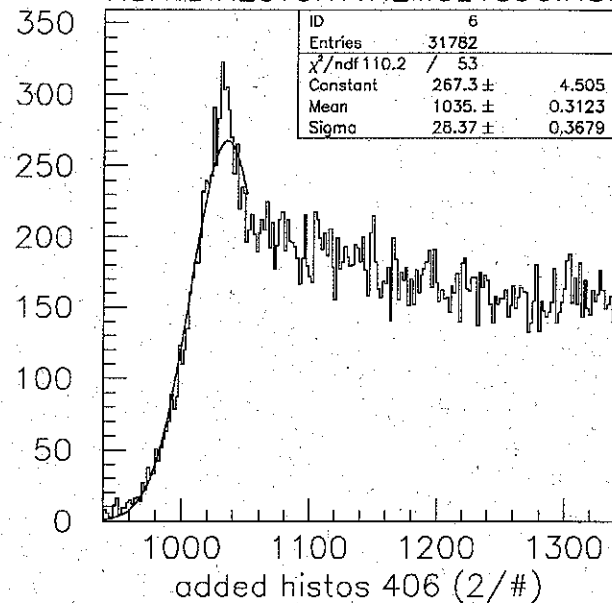
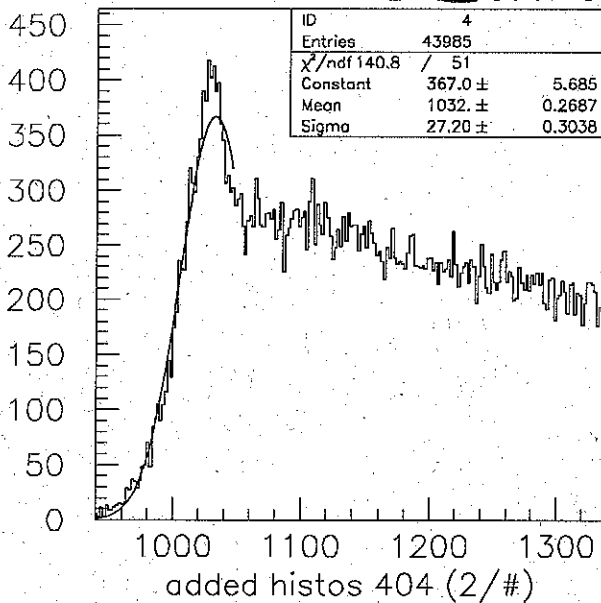
Figure 5a)

20/04/99 15.29

Run 1892-1896, 20kV, 100G, 400nm Au, no cut, Sample 0kV

HSN\$DIRECTORY:NEMUz1896.HSNz

HSN\$DIRECTORY:NEMUz1896.HSNz



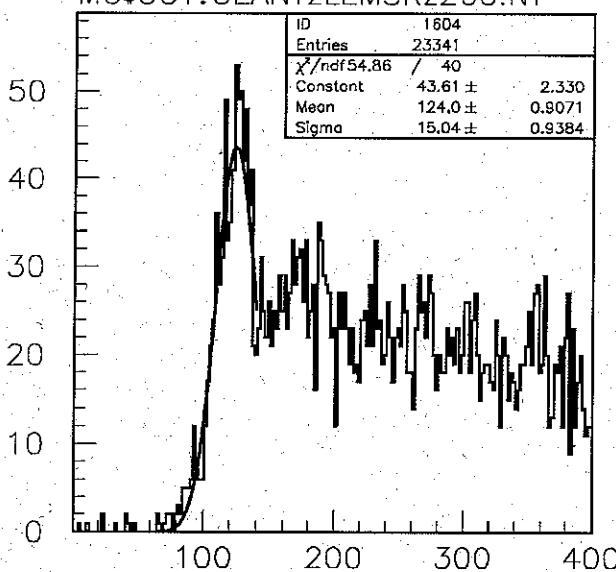
$$\bar{\sigma} = 29.5(1.0)_{\text{ns}}$$

Figure 5b)

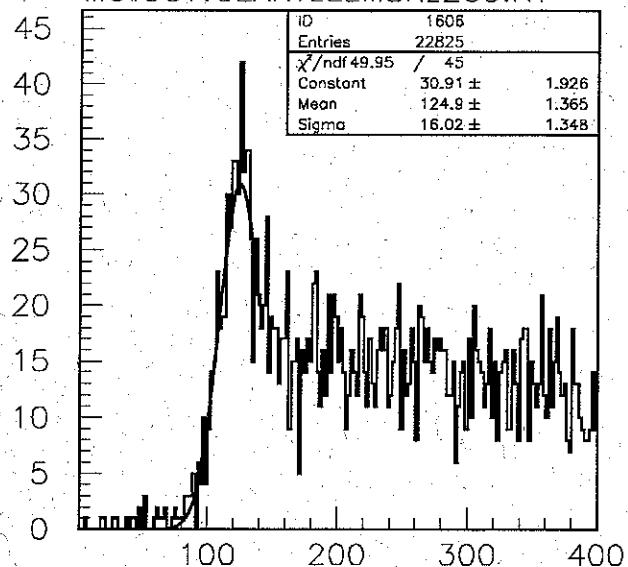
$\leq \sim 20 \text{ keV}$ am Moderator

20/04/99 16.25

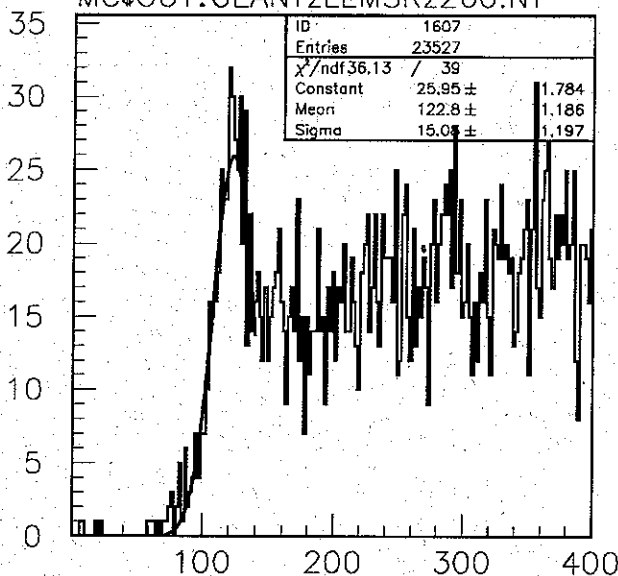
GEANT, $p=1.95 \text{ MeV}/c = 18 \text{ keV}$, $z_0 = -74 \text{ cm}$, $e^+ e^- \gamma$ 100keV, 50G, cryo
MC\$OUT:GEANTzLEMSRz260.NT



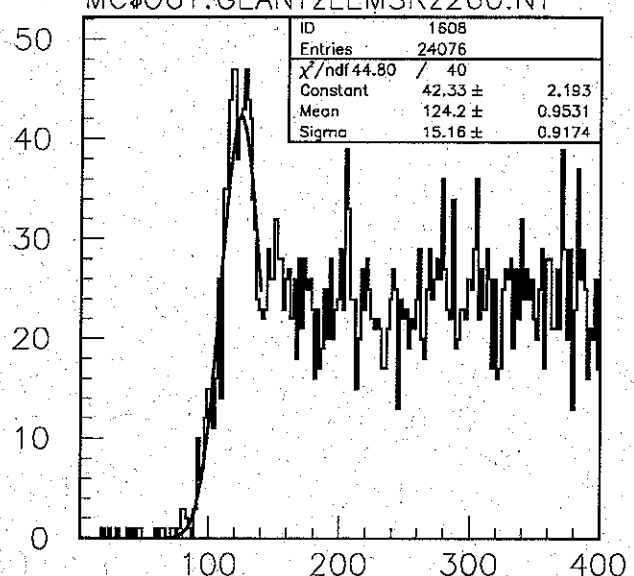
MC\$OUT:GEANTzLEMSRz260.NT



GEANT 260 left , e^+ or e^- bit, de gt 0, 2ns bins
MC\$OUT:GEANTzLEMSRz260.NT



GEANT 260 top , e^+ or e^- bit, de gt 0, 2ns bins
MC\$OUT:GEANTzLEMSRz260.NT



GEANT 260 right , e^+ or e^- bit, de gt 0, 2ns bins
GEANT 260 bottom, e^+ or e^- bit, de gt 0, 2ns bins

$t_0 = 133 \text{ ns}$ (time, when μ^+ hits MCP)

$\bar{\sigma} = 15.3(2) \text{ ns}$

$\bar{t}_{\text{mean}} = 124.0(4) \text{ ns}$

Figure 5c)

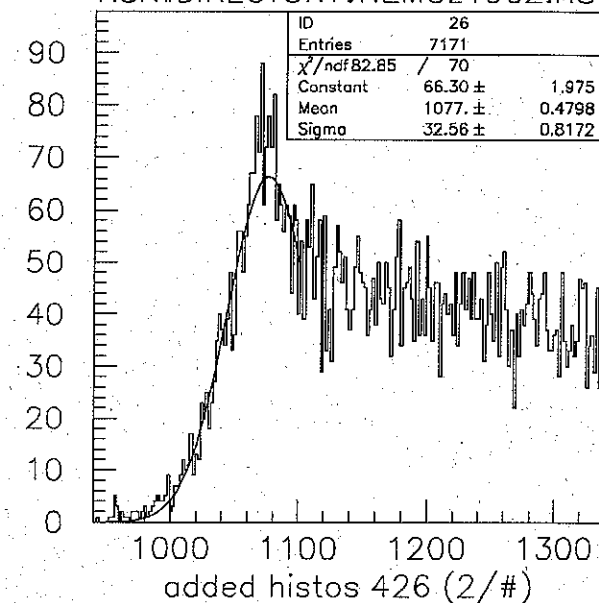
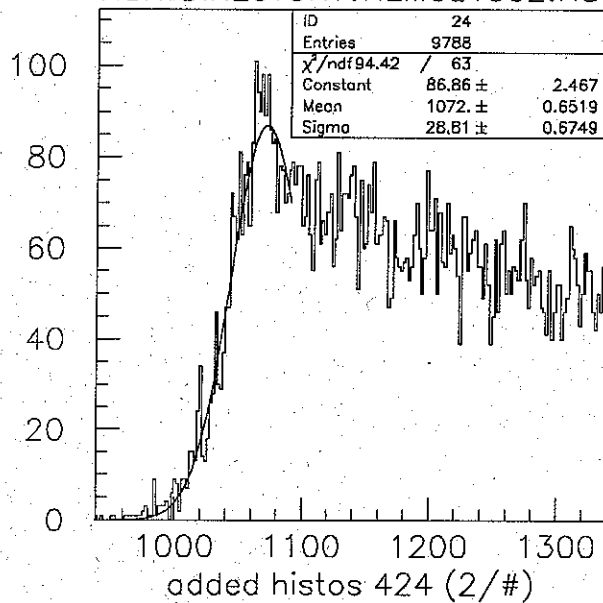
Sample = 0 kV

Run 1898–1902, 15 kV, 100 G, 400nm Au sample, Online M3S1 Cut (63–79)

20/04/99 14.43

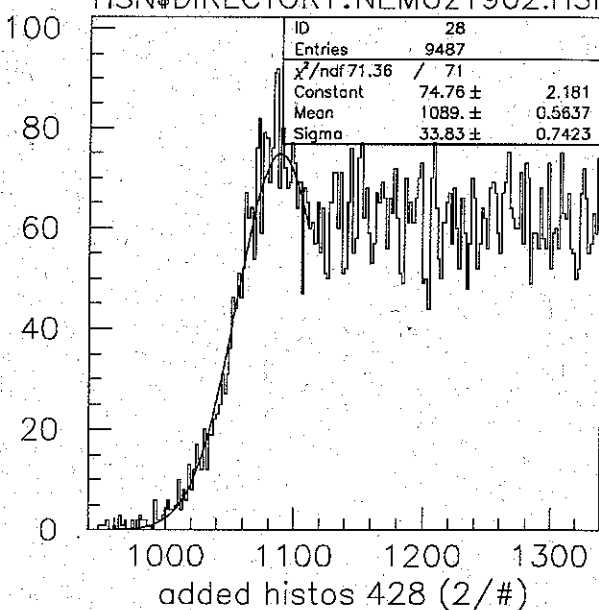
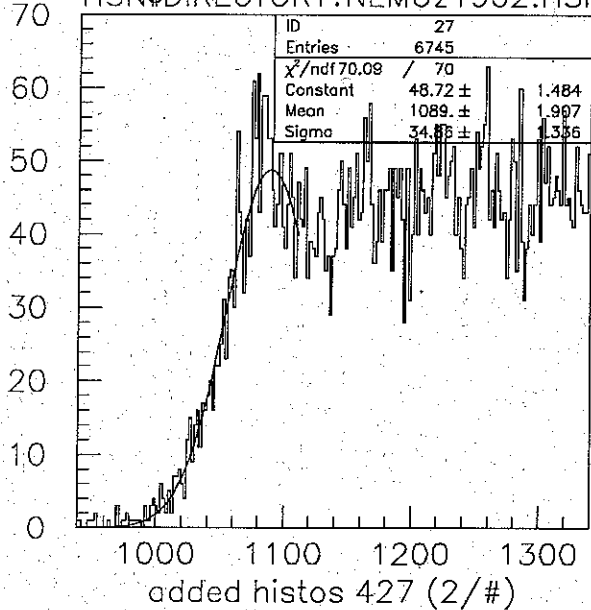
HSN\$DIRECTORY:NEMUz1902.HSNz

HSN\$DIRECTORY:NEMUz1902.HSNz



HSN\$DIRECTORY:NEMUz1902.HSNz

HSN\$DIRECTORY:NEMUz1902.HSNz



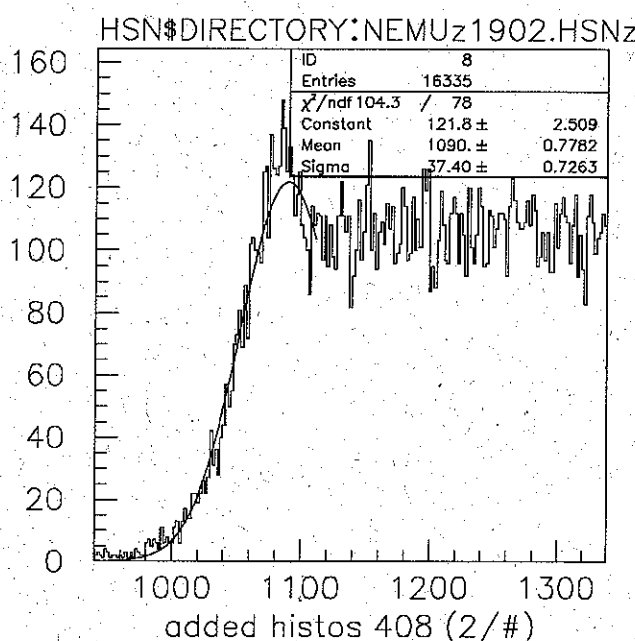
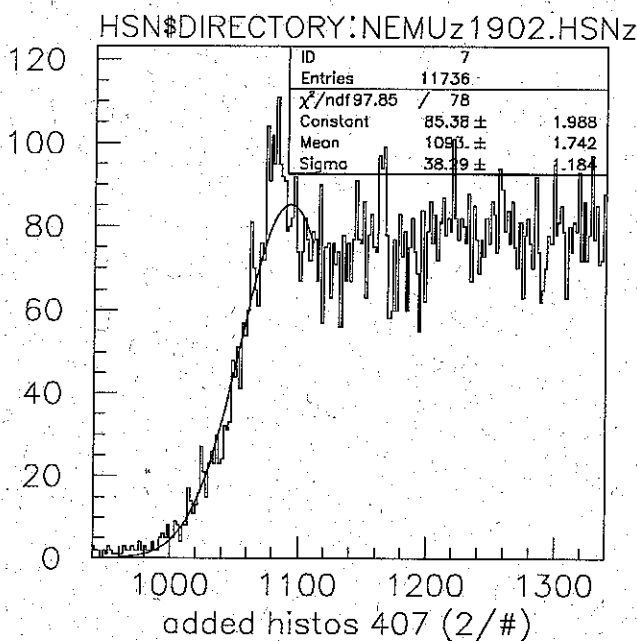
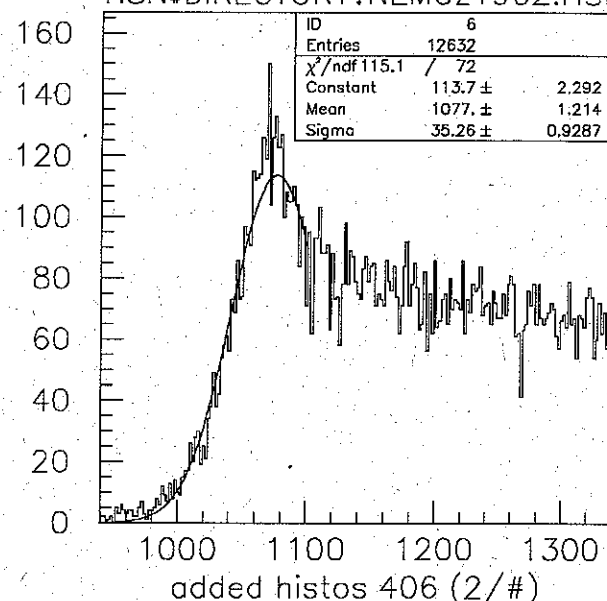
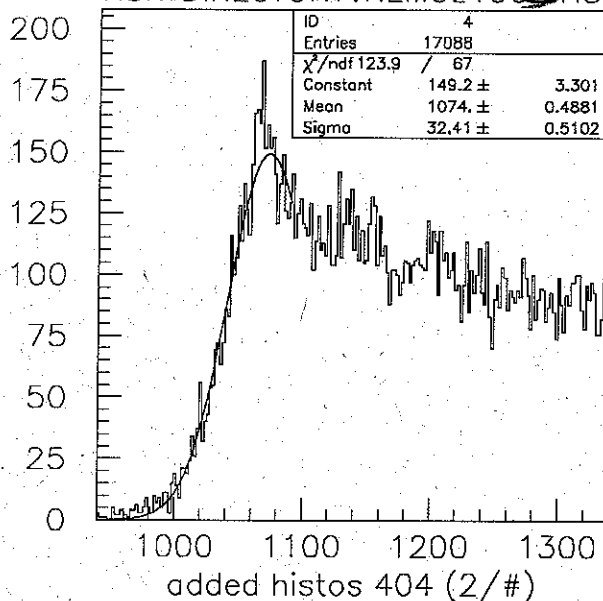
$$\bar{\sigma} = 33.5(1.3) \text{ ns}$$

Figure 6a)

Sample = 0 kV

Run 1898–1902, 15 kV, 100 G, 400nm Au sample no cut
HSN\$DIRECTORY:NEMUz1902.HSNz

20/04/98 14.44



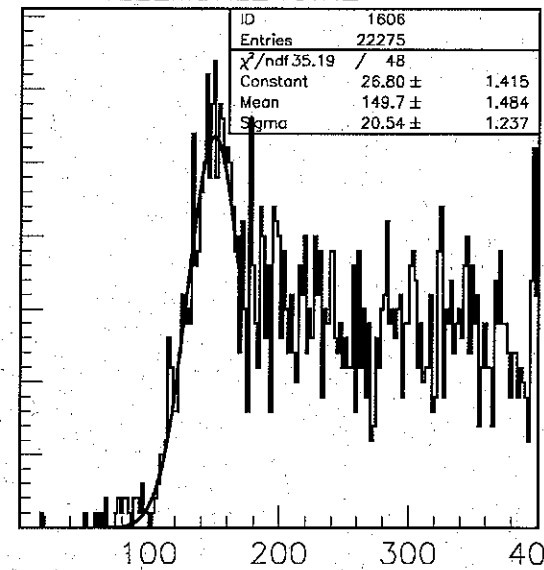
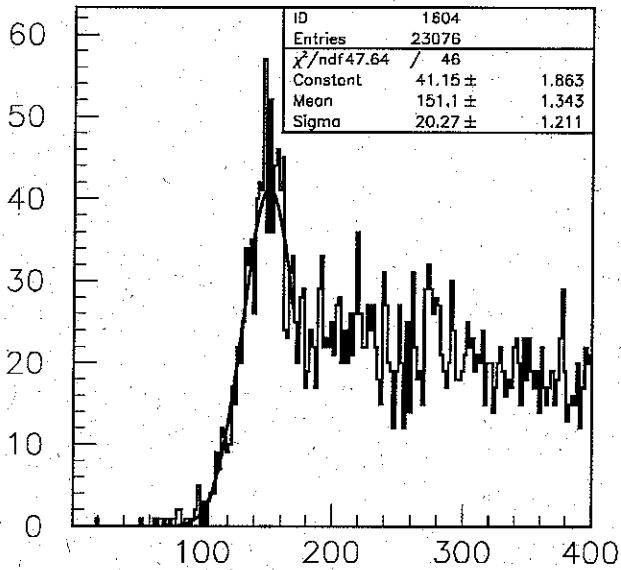
$$\bar{\sigma} = 35.9(1.3) \text{ ns}$$

Figure 65)

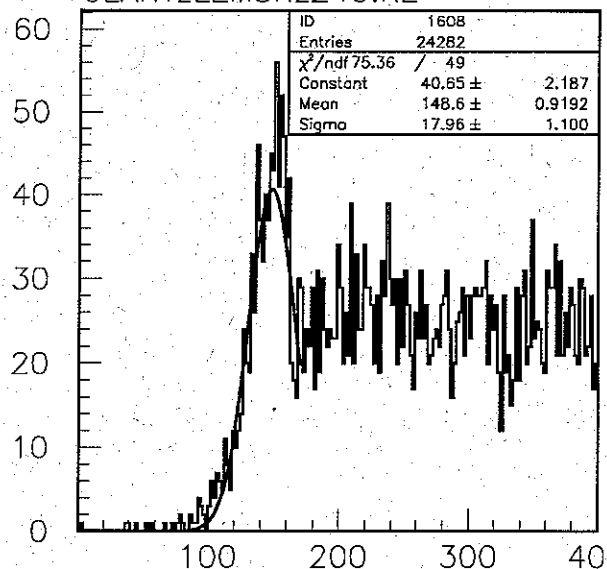
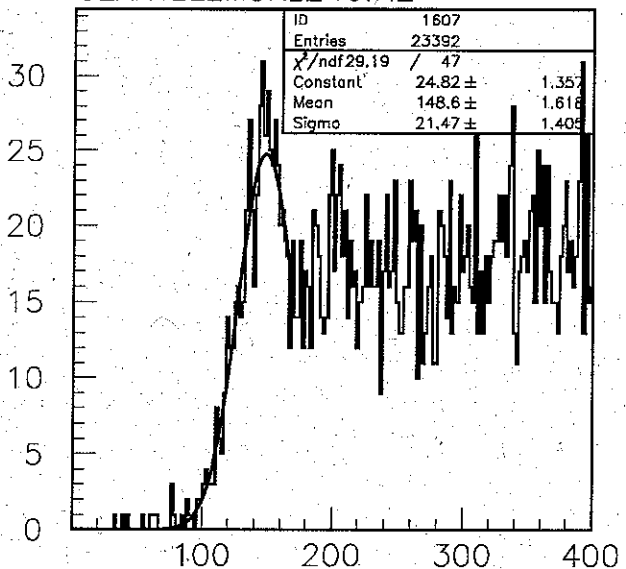
$\hat{z} \approx 15.1\text{V}$ an Moderator

20/04/99 16.27

GEANT, $p=1.62\text{MeV}/c=12.4\text{keV}$, $z_0=-74\text{cm}$, $e^+ e^- \gamma$ 100keV, 50G, cryo
GEANTzLEMSRz240.RZ



GEANT 240 left , e^+ or e^- bit, de gt 0, 2ns bins
GEANTzLEMSRz240.RZ



GEANT 240 right , e^+ or e^- bit, de gt 0, 2ns bins
GEANT 240 bottom, e^+ or e^- bit, de gt 0, 2ns bins

Fitted gaussian (χ^2 minimization) to 'broad peak'.

$t_0 = 164\text{ns}$ (time, when p⁺ hits MCP)

$\bar{\sigma} = 20.1(8)\text{ns}$ Mean = $149.5(6)\text{ns}$

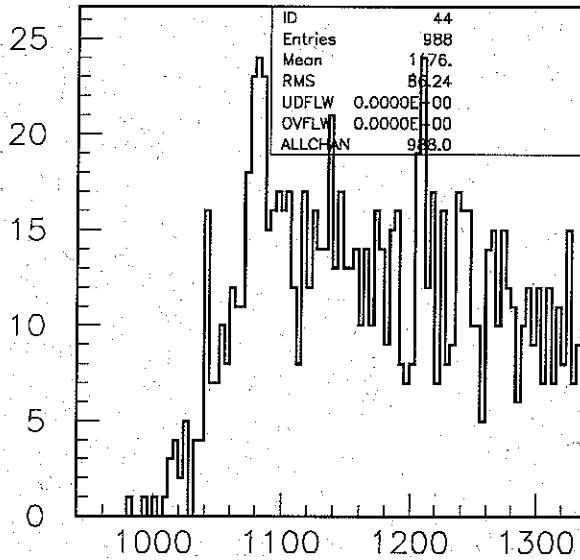
Fig. 6c)

Run XI data:

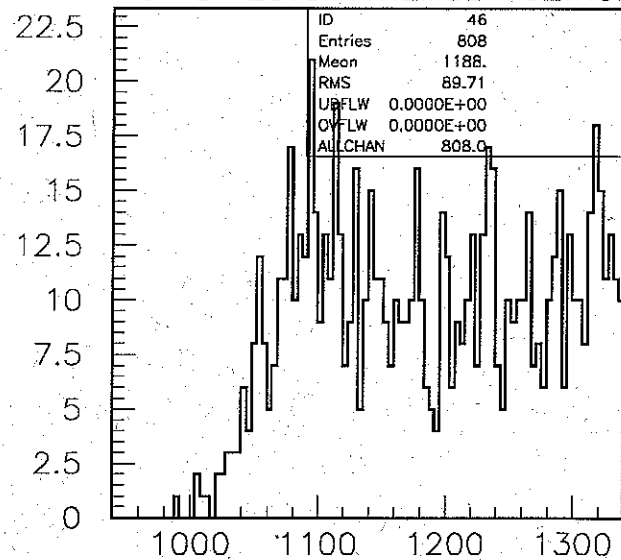
115 I.V., 100g, MCP2

20/04/99 13.46

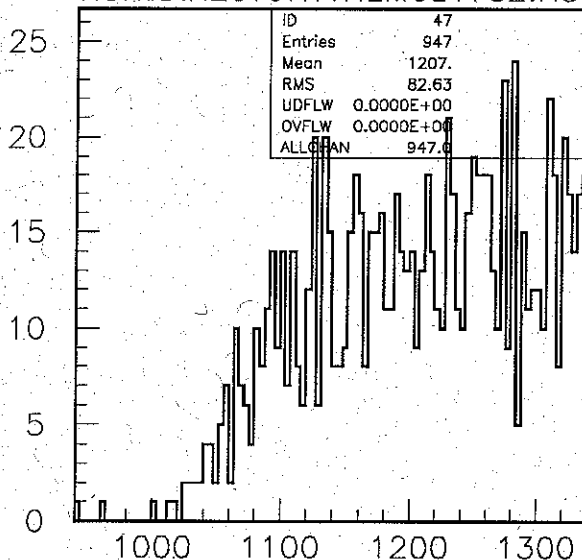
HSN\$DIRECTORY:NEMUz1732.HSNz



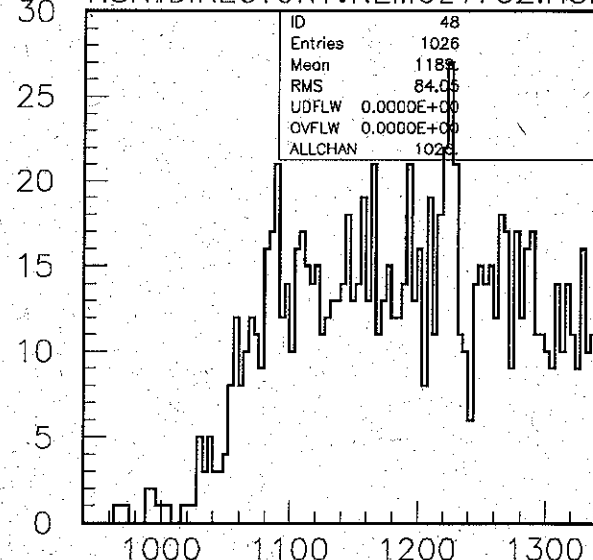
HSN\$DIRECTORY:NEMUz1732.HSNz



1732, left, 115 le m3s1 le 126 (4/#)
HSN\$DIRECTORY:NEMUz1732.HSNz



1732, top, 115 le m3s1 le 126 (4/#)
HSN\$DIRECTORY:NEMUz1732.HSNz



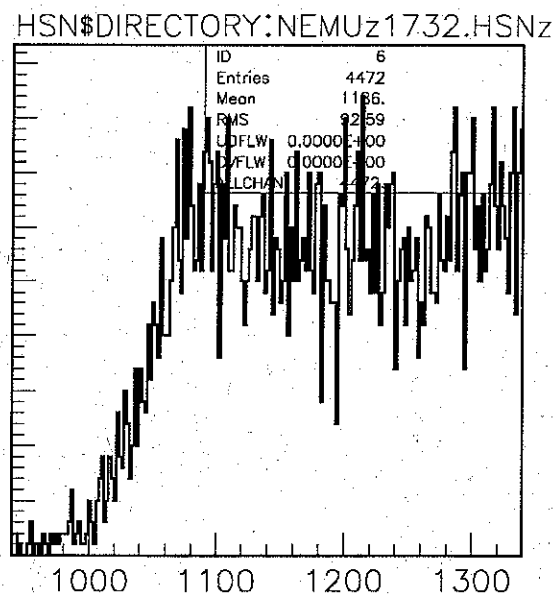
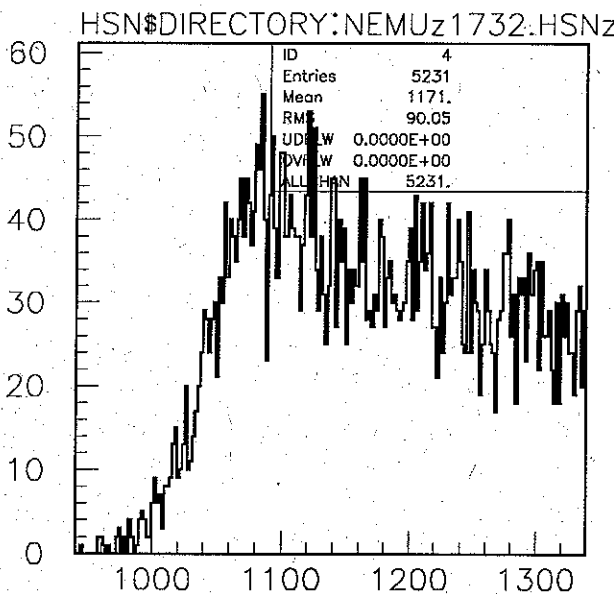
1732, rite, 115 le m3s1 le 126 (4/#)

T0F cut m3s1 $\in [115, 126]$, start pt peak

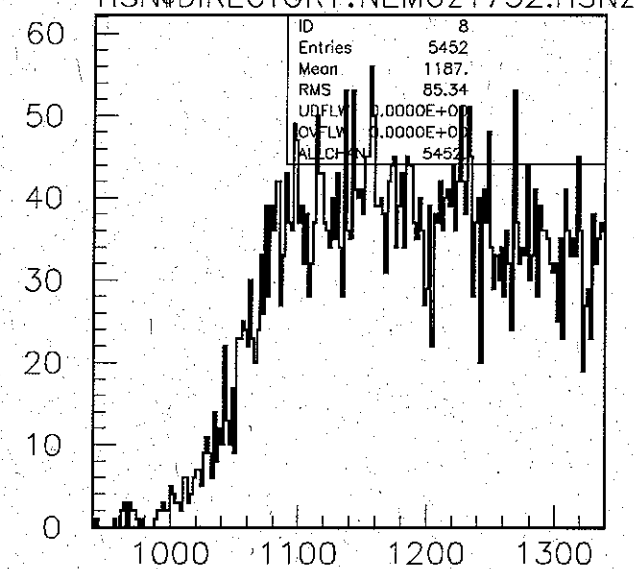
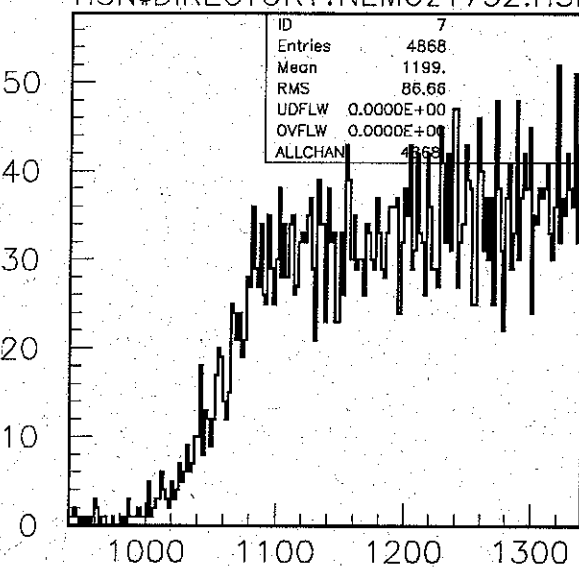
Figure 7a)

15kV, 100g, MCP2

20/04/99 13.44



1732, Left. (M3-triggered) (TDC4208-4) (2/32), Top (M3-triggered) (TDC4208-6) (2/#)

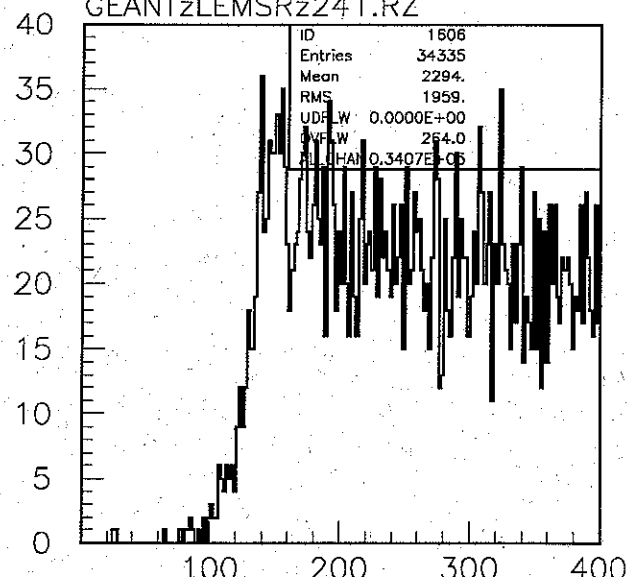
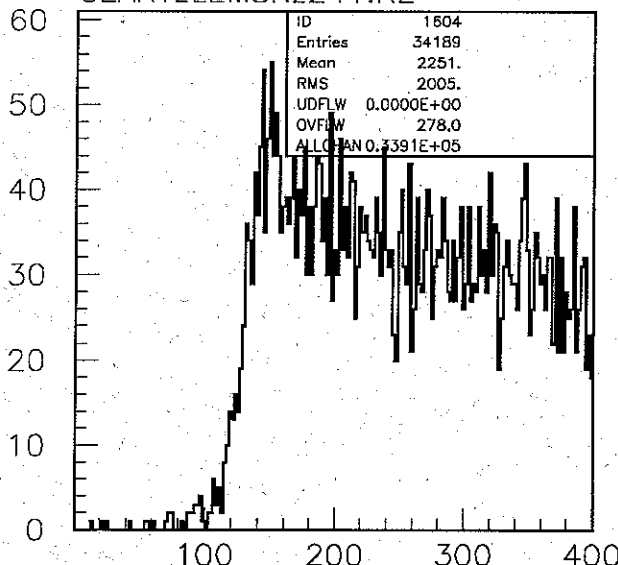


1732, Right. (M3-triggered) (TDC4208-7) (23/24) Bottom (M3-triggered) (TDC4208-8) (2/#)

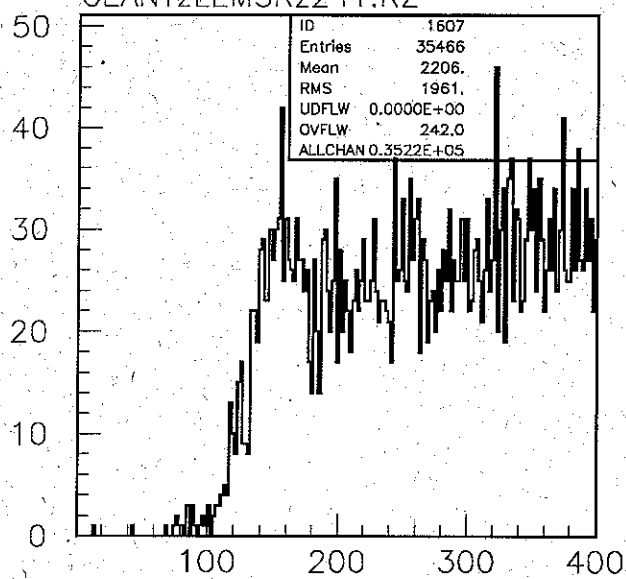
Figure 7b)

20/04/99 14.07

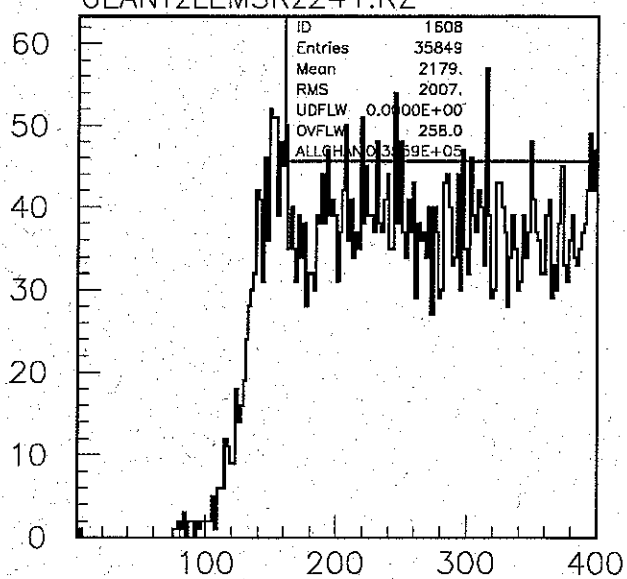
GEANT, $p=1.62\text{MeV}/c=12.4\text{keV}$, $z_0=-74\text{cm}$, e^+ , e^- , γ 100keV, 50G, MCP2
GEANTzLEMSRz241.RZ



GEANT 241 left, e+ or e- bit, de > 0, 2ns bins
GEANTzLEMSRz241.RZ



GEANT 241 top, e+ or e- bit, de > 0, 2ns bins
GEANTzLEMSRz241.RZ



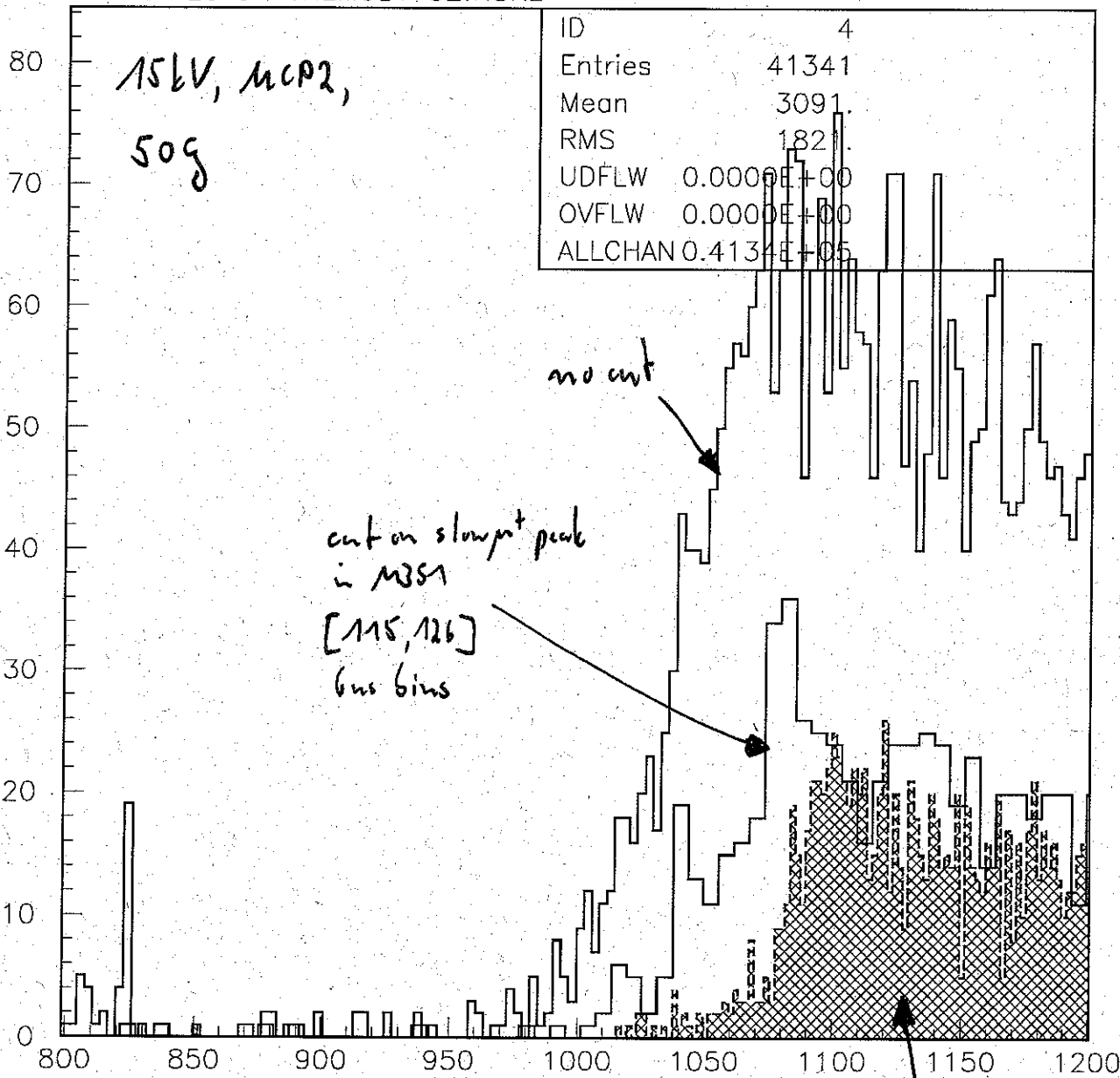
GEANT 241 right, e+ or e- bit, de > 0, 2ns bins

GEANT 241 bottom, e+ or e- bit, de > 0, 2ns bins

Figure 7c)

20/04/99 13.34

HSN\$DIRECTORY:NEMUz1732.HSNz



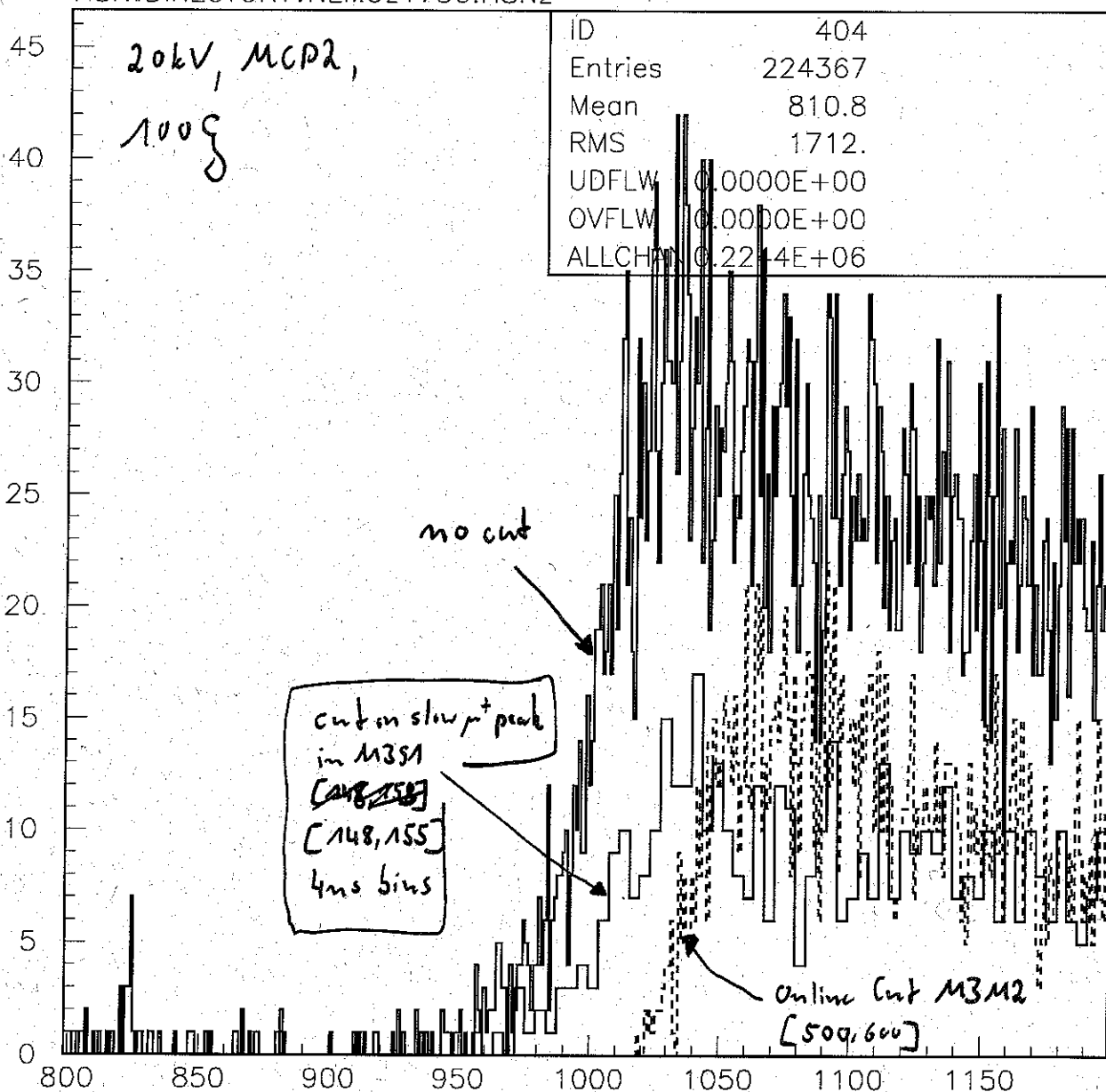
Online cut
M3M2 < [500,600]

2 ns bins

Fig 8a)

20/04/99 12.16

HSN\$DIRECTORY:NEMUz1736.HSNz



1736, Left (M3-triggered) (TDC4208-4)

Fig 86

20/04/99 13.13

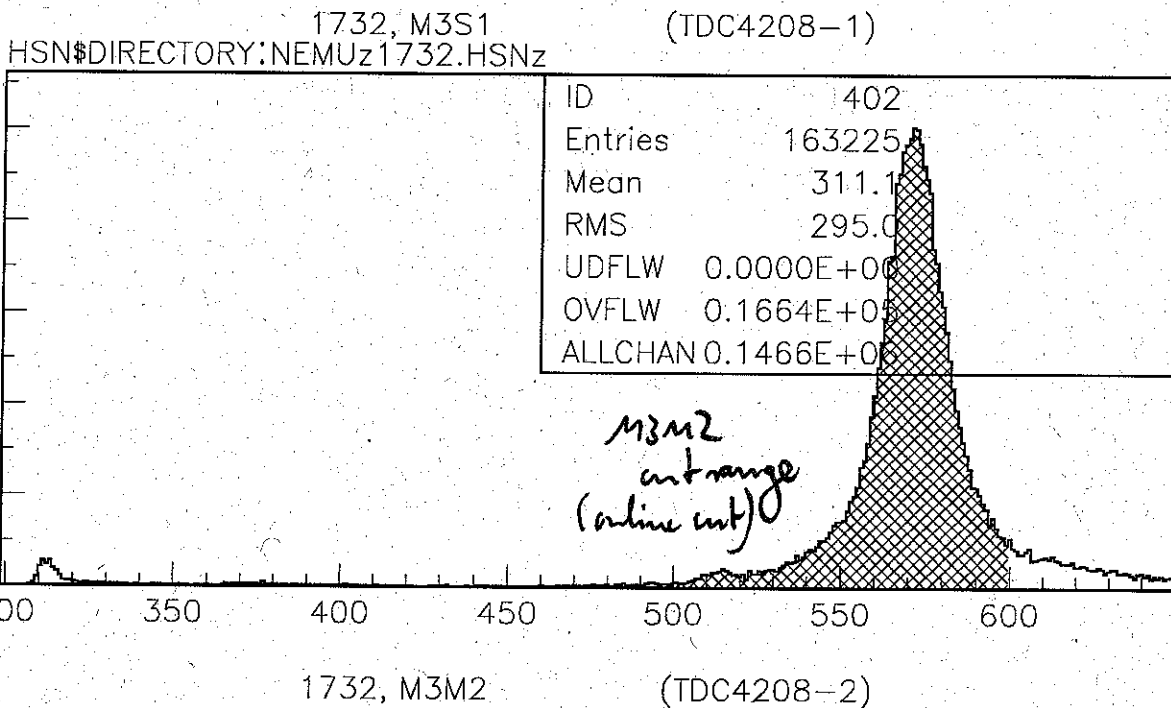
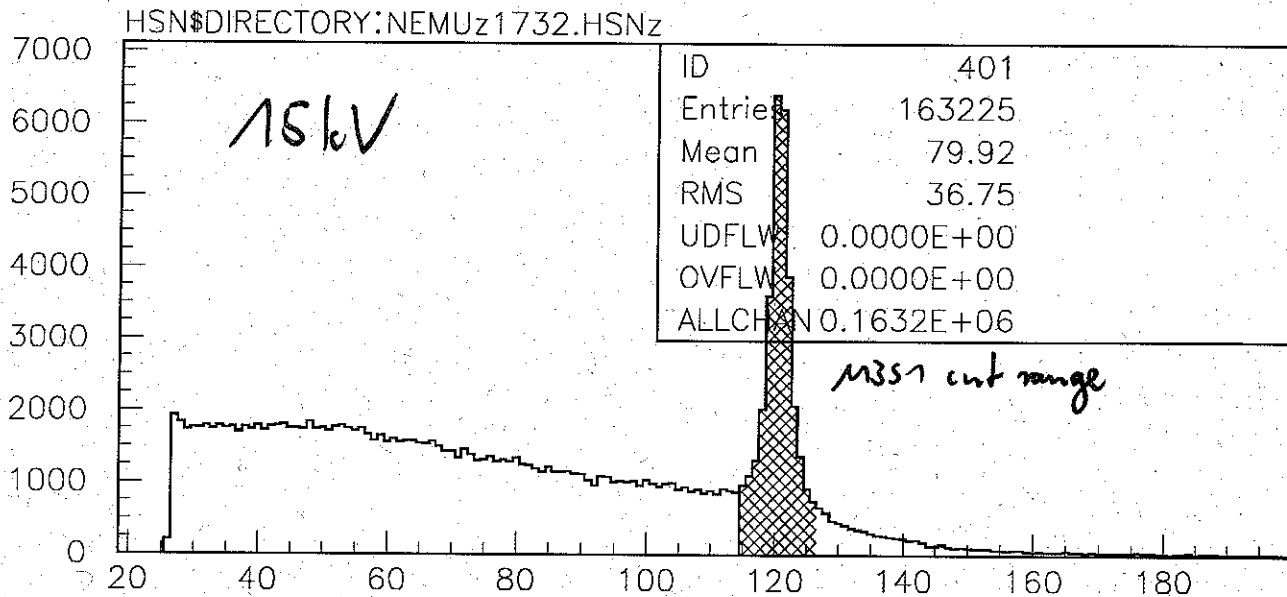
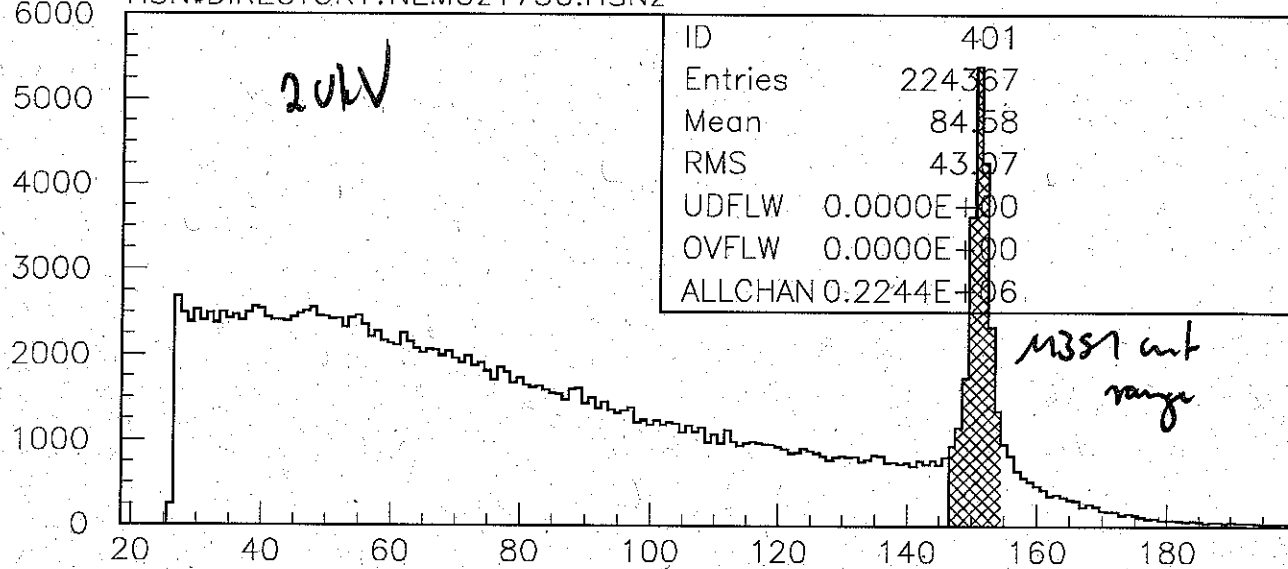


Fig. 8c)

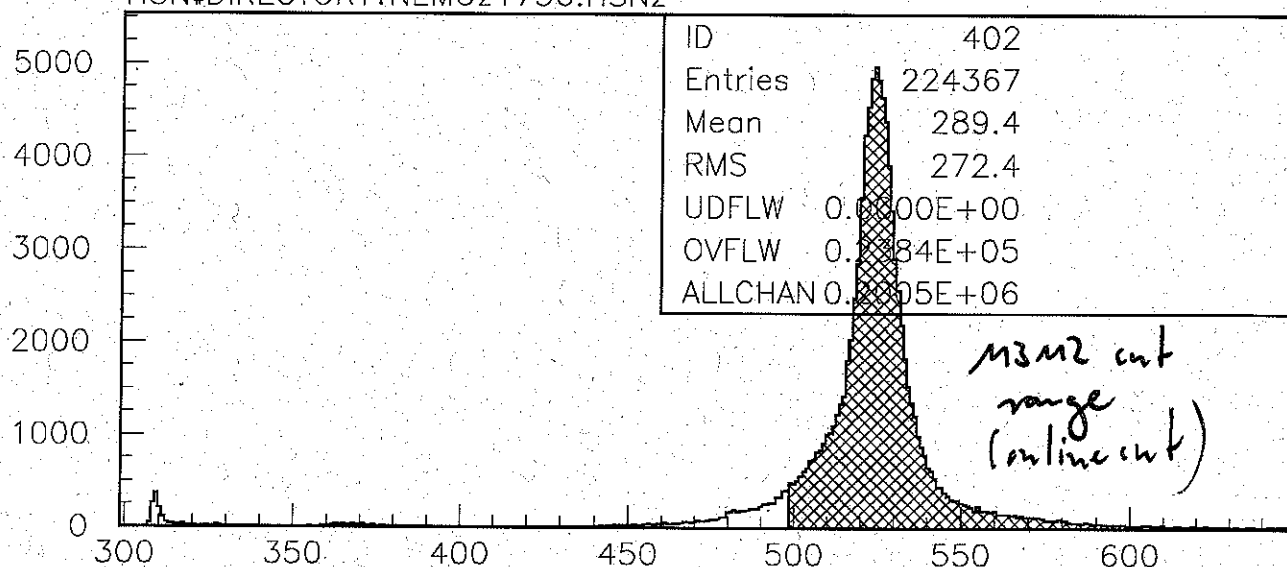
20/04/99 12.46

HSN\$DIRECTORY:NEMUz1736.HSNz



1736, M3S1
HSN\$DIRECTORY:NEMUz1736.HSNz

(TDC4208-1)



1736, M3M2

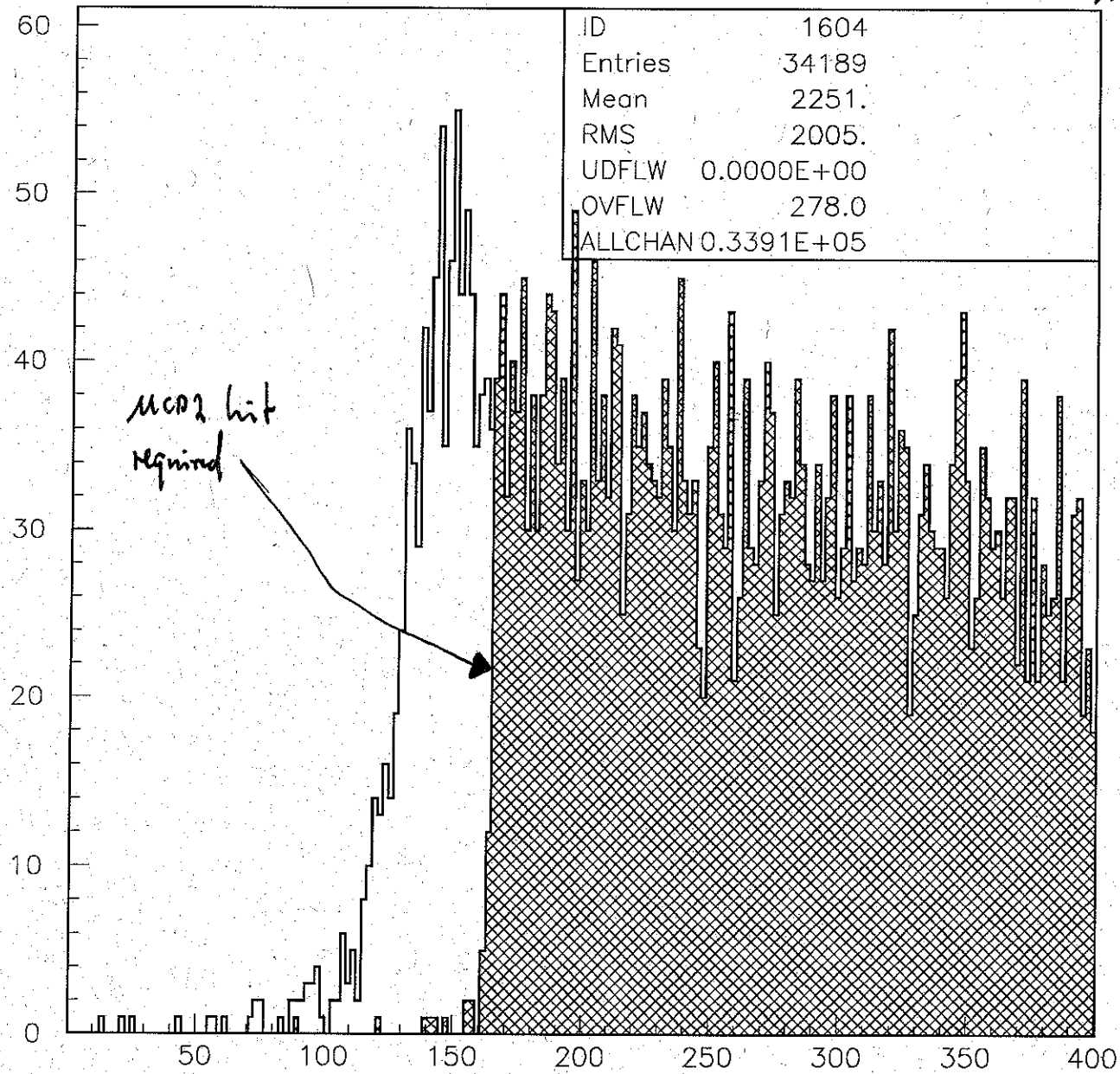
(TDC4208-2)

| Fig 8d |

20/04/99, 14.03

GEANT, $p=1.62\text{MeV}/c=12.4\text{keV}$, $z_0=-74\text{cm}$; e^+ , e^- , γ 100keV, 50G, Run XI
GEANTzLEMSRz241.RZ

MCP2



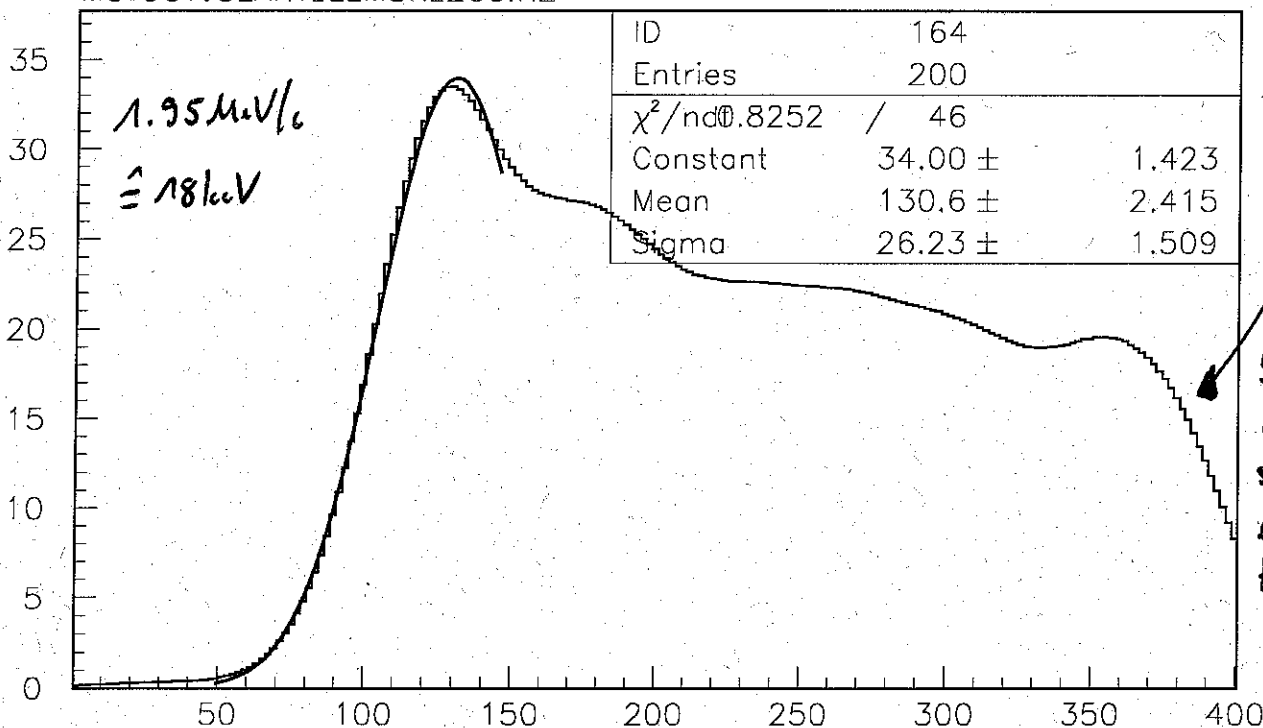
GEANT 241 left , e^+ or e^- bit, de gt 0, 2ns bins

| Fig 8e)

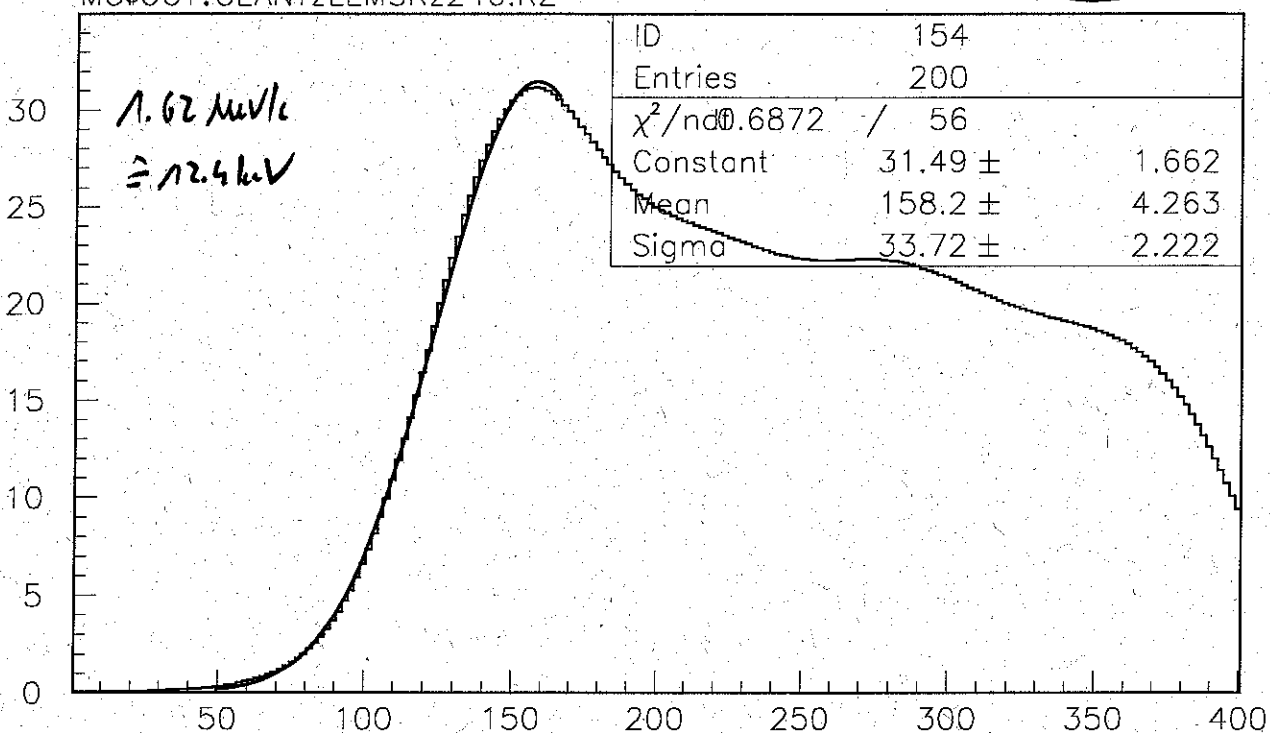
Run XI, Cryo

21/04/99 14.34

GEANT, folded decay spectra 20 kV (Top) and 15 kV (Bottom)
MC\$OUT:GEANTzLEMSRz260.RZ



GEANT 260 left , e+ or e- bit, de > 0, 2ns bins (2/#), $\sigma_{fold} = 16 \text{ ns}$
MC\$OUT:GEANTzLEMSRz240.RZ



GEANT 240 left , e+ or e- bit, de > 0, 2ns bins (2/#), $\sigma_{fold} = 22 \text{ ns}$

Figure 9

20/04/99 15.48

GEANT, Beamspot $\phi=1\text{cm}$ homogenous, N_L/N_R in dependence of x shift

